2015

A New Islanding Detection Method Based On Wavelet-transform and ANN for Inverter Assisted Distributed Generator

Zhengyuan Guan
University of Kentucky, gzyily1990@gmail.com

STUDENT AGREEMENT:

I represent that my thesis or dissertation and abstract are my original work. Proper attribution has been given to all outside sources. I understand that I am solely responsible for obtaining any needed copyright permissions. I have obtained needed written permission statement(s) from the owner(s) of each third-party copyrighted matter to be included in my work, allowing electronic distribution (if such use is not permitted by the fair use doctrine) which will be submitted to UKnowledge as Additional File.

I hereby grant to The University of Kentucky and its agents the irrevocable, non-exclusive, and royalty-free license to archive and make accessible my work in whole or in part in all forms of media, now or hereafter known. I agree that the document mentioned above may be made available immediately for worldwide access unless an embargo applies.

I retain all other ownership rights to the copyright of my work. I also retain the right to use in future works (such as articles or books) all or part of my work. I understand that I am free to register the copyright to my work.

REVIEW, APPROVAL AND ACCEPTANCE

The document mentioned above has been reviewed and accepted by the student's advisor, on behalf of the advisory committee, and by the Director of Graduate Studies (DGS), on behalf of the program; we verify that this is the final, approved version of the student's thesis including all changes required by the advisory committee. The undersigned agree to abide by the statements above.

Zhengyuan Guan, Student

Dr. Yuan Liao, Major Professor

Dr. Caicheng Lu, Director of Graduate Studies

A New Islanding Detection Method Based On Wavelet-transform and ANN for Inverter Assisted Distributed Generator

---

THESIS

A thesis submitted in partial fulfillment of the
requirements for the degree of Master of Science in Electrical Engineering
in the College of Engineering
at the University of Kentucky

By

Zhengyuan Guan

Lexington, Kentucky

Director: Dr. Yuan Liao, Professor of Electrical and Computer Engineering

Lexington, Kentucky

2015

ABSTRACT OF THESIS

A NEW ISLANDING DETECTION METHOD BASED ON WAVELET-TRANSFORM AND ANN FOR INVERTER ASSISTED DISTRIBUTED GENERATOR

Nowadays islanding has become a big issue with the increasing use of distributed generators in power system. In order to effectively detect islanding after DG disconnects from main source, author first studied two passive islanding methods in this thesis: THD&VU method and wavelet-transform method. Compared with other passive methods, each of them has small non-detection zone, but both of them are based on the threshold limit, which is very hard to set. What's more, when these two methods were applied to practical signals distorted with noise, they performed worse than anticipated.

Thus, a new composite intelligent based method is presented in this thesis to solve the drawbacks above. The proposed method first uses wavelet-transform to detect the occurrence of events (including islanding and non-islanding) due to its sensitivity of sudden change. Then this approach utilizes artificial neural network (ANN) to classify islanding and non-islanding events. In this process, three features based on THD&VU are extracted as the input of ANN classifier. The performance of proposed method was tested on two typical distribution networks. The obtained results of two cases indicated the developed method can effectively detect islanding with low misclassification.

KEYWORDS: Distribution generation (DGs), islanding detection, wavelet-transform, artificial neural network (ANN).

Zhengyuan Guan

Signature

5/8/2015

Date

A NEW ISLANDING DETECTION METHOD BASED ON WAVELET-TRANFORM AND ANN FOR INVERTER ASSISTED DISTRIBUTED GENERATOR

By

Zhengyuan Guan

Yuan Liao

(Director of Thesis)

Caicheng Lu

(Director of Graduate Studies)

5/8/2015

(Date)

ACKNOWLEDGEMENTS

I would never have been able to finish my thesis without the guidance of my committee members, help from my friends, and support from my family.

I would like to express the deepest appreciation to my thesis advisor and committee chair, Professor Yuan Liao, for his careful guidance, patience, and providing me a good laboratory for doing research. I would also like to thank Prof. Paul Dollof and Prof. Yu-ming Zhang, be my committee member and take part in my thesis defense. They gave me a lot of advices and pointed out many drawbacks of my thesis after thesis presentation. Special thanks go to Dr. Guangbin Zhang, who gave me many helps and taught me many basic skills to write a graduation thesis.

I would like to thank my friend, Jin Chang, who inspired me to use wavelet-transform to solve the problem in this thesis. I would also like to thank to Jie Chen, Zhaofeng Wang, Wanjin Xiu, Xiang Li, who as good friends, were always willing to help. It would have been a lonely lab without them.

I would also like to thank my parents and my uncle, who were always standing by my side and giving their best efforts and wishes to support me achieve my degree.

TABLE OF CONTENTS

LIST OF TABLES

LIST OF FIGURES

Chapter 1 Introduction

1.1 Background

Nowadays, micro-grid systems have become an important role in meeting the needs of environmental requirements like reducing the emissions of greenhouse gases and also coping with the rising traditional energy prices like coals, natural gas and hydro generation. Micro-grid generation can include photovoltaic (solar farm), wind generation, fuel cells or other generation types. The use of these distributed generations can effectively lower environmental impacts, improve the safety of power supply and decrease the pressure of power supply in the peak time [1]. However, islanding operation is the most important concern when using the DGs. Islanding can be explained by Fig 1.1, if the circuit breaker is tripped due to the occurrence of fault, the remaining local load may be kept powering by DG. This phenomenon is called islanding [2].

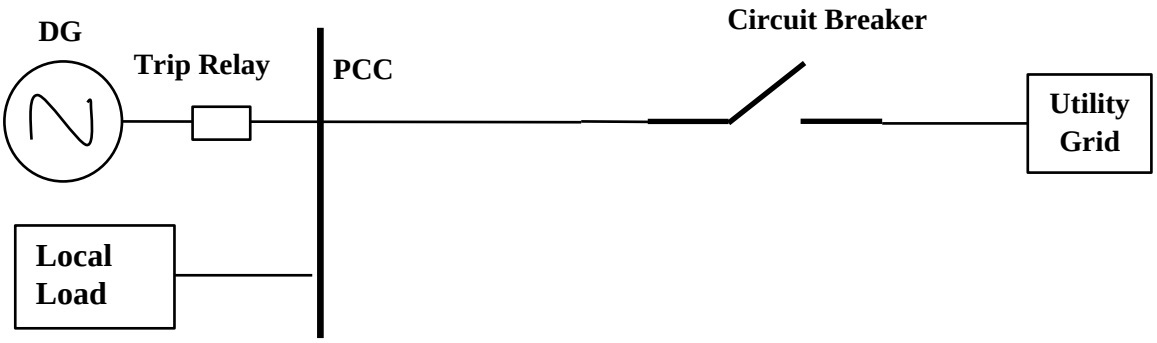

Figure 1.1 Islanding Operation for DG system

Islanding has many negative impacts on utility power system, such as [2]:

1. Damage to the utility workers who may not realize the DG is still powering the local load.

2. Huge damages to the DG itself when DG is reconnected to grid.
3. Resulting a poor power quality because of the unregulated voltage and frequency after islanding.

Because of listed reasons, DGs must install anti-islanding protection devices in order to detect islanding as soon as possible when the utility power is interrupted abruptly, and disconnect DGs with the network quickly and accurately (less than 2 sec), required by the IEEE 929-1988 [3] and IEEE 1547-2003 [4] standard. IEEE 1547-2003 also gives the specified clearing time for abnormal voltage and frequency. Both standards have been shown in Table 1.1 and Table 1.2.

Table 1.1 Interconnection system response to abnormal voltage [3] [4]

Voltage Range (% of the base voltage)	**Clearing time**
V<60	6 cycles
60≤V<106	120 cycles
106≤V<132	Normal
132≤V<165	120 cycles
165≤V	6 cycles

(a) IEEE Std 929

Voltage Range (% of the base voltage)	**Clearing time**
V<60	0.16s
60≤V<106	2.0s
106<V<132	Normal Operation
132≤V<144	1.0s
144≤V	0.16s

(b) IEEE Std 1547

Table 1.2 Interconnection system response to abnormal frequency [4]

DR size	**Frequency range (Hz)**	**Clearing time (s)**
≤30 kW	>60.5	0.16
	<59.3	0.16
>30 kW	>60.5	0.16
	<{59.8 to 57.0} (adjustable set point)	Adjustable 0.16 to 300
	<57.0	0.16

1.2 **Literature review**

The following includes a detailed description of different islanding detection methods currently proposed in many other literatures. In general, islanding detection method can be divided into two groups: remote techniques and local techniques. Several examples of these techniques are presented to review their characteristics as a preliminary knowledge for this thesis.

1.2.1 Remote technique

Remote techniques can be classified as Power line communication (PLC), supervisory control and data acquisition (SCADA), and transfer trip (TT), which send signals from the grid to DG continuously. For example, PLC scheme uses a signal generator as the main devices installed at the secondary side of the substation, and this generator will continuously send signals to all the signal detectors installed at the end of DGs, which will receive the signals from signal generator. If the signal receiver does not sense any signal, it means an islanding condition is formed and the DG will be tripped

immediately. So as to the TT scheme, the main idea of this method is to monitor every circuit breaker that may cause an islanding for DG. If a disconnection happens in distribution network, a central algorithm decides which DG needs to be islanded and sends the signal to trip this DG. However, although remote techniques are quite reliable for islanding detection, but they are very expensive because you need to monitor every point in the distribution network where a disconnection may happen. [5] [6] [7].

1.2.2 Local technique

For Local techniques also can be classified as two sub-types: active techniques and passive techniques. Unlike remote techniques, local techniques utilize the system parameters like voltage magnitude and frequency at the DG end for islanding detection.

The active technique, such as reactive power export error detection, impedance measurement method, phase (or frequency) shift methods, slip-mode frequency shift algorithm (SMS) and active frequency drift with positive feedback method (AFDPF), has faster response time and small non detection zone (NDZ). For example, for impedance measurement techniques, the inverter sends a signal into the output current and the voltage response at the DG end is monitored. If inverter output circuit impedance shows low impedance value, we can say an islanding is detected because the low circuit impedance is caused by the distribution network disconnection. However, as it says, it introduces some external signal into the power system so that this technique may reduce the power quality, as well as other active techniques [8] [9]. This is the main drawback of active techniques already proposed.

Compared with active technique, the main advantage of passive technique is that it does not affect the normal operation of DG which means it will not introduce any

disturbances into system. Mostly we will set a threshold value for monitoring parameters as a principle to determine islanding (like voltage we mostly set as 85%-110% of normal value). However, the selection threshold is a big issue for single parameter based passive techniques.

Different passive islanding detection techniques have been widely documented in many papers by measuring system parameters such as frequency (f), voltage magnitude (U), current (I), the rate of change of frequency ($ROCOF$), the rate of change of voltage ($ROCOV$), rate of change of power ($ROCOP$), change in power factor (pf), the vector surge technique, the phase shift method, voltage vector shift (VVS), rate of change of power angle difference ($ROCPAD$) [10] [11] [12].

Over/Under Voltage Protection (OVP/UVP) The voltage magnitude varies with the changes in reactive power unbalance between generation and demand [13]. Therefore, abnormal variation of voltage magnitude can be treated as a signal to detect islanding. As for the voltage protection relay, trip signal can be sent if the voltage magnitude reaches standard requirements in Table 1.1-1.2.

Over/Under Frequency Protection (OFP/UFP) When islanding happens, the active power unbalance between the generation and demand may affect the generator speed, causing the change of frequency. The OFP/UFP relays can disconnect the DG from utility grid when measured frequency exceeds or is under a preset threshold.

Rate of Change of Frequency (ROCOF) If the value of the rate of change of frequency exceeds the preset threshold, ROCOF relay sends a trip signal. Typically the ROCOF setting for the 60Hz power systems are between 0.1 and 1.2 Hz/s [10].

Voltage Vector Shift (VVS) When islanding is formed due to the loss of grid connection, as a result, the cycle length of the terminal voltage waveform is changed. The change of cycle length is based on the active power mismatch between the local load and DG output power. VVS method measures the difference between the current cycle duration with the referenced cycle duration. Then this difference can be expressed as an angle, which can be compared with the preset angle threshold. If the angle exceeds the threshold, a tripping signal is sent from the relay and the circuit breaker is open. A detailed analysis of VVS method can be found in [10].

Rate of Change of Power Angle Difference (ROCPAD) The process of this method is like this: first the voltage and current at the DG end is monitored and the phasor is calculated by synchronous transformation based algorithm. Then power angle difference can be estimated and ROCPAD also can be generated to detect islanding [12].

However, large non-detection-zone (NDZ) is a main common drawback of these methods. NDZ is defined as the range of local load power setting which causes the islanding detection methods fail to detect islanding in most conditions. That means if the load power and distributed generator nominal power is closely matched, the passive islanding detection methods will fail to detect islanding operation since the changes monitoring parameters are still within the allowed threshold limit.

1.3 Recent Research Status

Islanding is also a cutting-edge research topic in power system or smart grid. In order to understand recent research status, author reviewed many other methods proposed in 2014. For example, in [14] the authors proposes 2 new DG control strategies providing frequency and voltage support via conventional droop slopes.

Reference [15] specifically designs a new wavelet filter WGM1.0 for islanding detection, associated with a new voltage-based index and corresponding energy of the change of the wavelet coefficients of the mean voltage. Then by using two machine learning classifier SVM and ETC, islanding is detected based on the calculated voltage index and the new wavelet. The result reflects the high adaptability of WGM1.0 for islanded signal pattern.

Reference [16] proposes a new universal islanding detection method which has three main phases including feature extraction, feature selection, and classification. First 21 possible features are extracted from the voltage and current waveforms, and then a sequential feature selection algorithm is applied to determine the features used in classification. Last, a random forest classifier is used to distinguish islanding and non-islanding. The test results show it has better performance than any other classifiers and has a fast detection response.

Reference [17] designs two dynamic estimators based on the amplitude and phase angles of the current injected by the grid at PCC in addition to the DG's local bus voltage. The simulation result shows the proposed method has small NDZ and short detection time. A algorithm is also developed for multi-DG power system.

Reference [18] provides the original records of distributed generation unintentional islanding events, which is very important for anti-islanding study but rarely documented in previous literature. This first-hand information can serve as credible references for DG planning and operation decision making.

Reference [19] proposes a multi-feature-based SVM classification technique to detect islanding, especially under critical islanding cases where VS relays fail to trigger.

A main advantage of this paper over others is that this paper considers islanding events in the presence of constant Z, constant I, and constant P load.

1.4 Thesis Objectives and Outline

After reviewing large number of current literature, author finds NDZ and threshold setting is still a big issue for islanding detection. In order to decrease the influence of NDZ, author found another two passive methods: islanding detection based on total harmonic distortion (THD) and voltage unbalance (VU) [20], and islanding detection based on the discrete wavelet analysis of the voltage measured at the end of DG [21] in other two papers. Then author tested the methods in MATLAB platform to see their performances. The result shows the new methods mainly have two advantages over conventional detection methods: they not only reduce the NDZ but without introducing any new disturbances so that won't affect the output power quality. However, it is still extremely hard to choose accurate threshold settings for these two methods to avoid mal-operation of trip relay due to some normal transient disturbance or noise, which may also produce sufficient variations of these parameters to reach the threshold setting. Therefore, inspired by [15], author proposed a new reliable composite method combined with THD&VU, wavelet-transform and artificial neural network (ANN) technique, solving this problem effectively. The newly proposed method was tested with a large number of islanding and non-islanding cases. The test results show this method correctly detect islanding with high level of accuracy where conventional methods fail to detect or mal-operate. Simulations were carried out by MATLAB/Simulink software and achieved in a 100 kW photovoltaic DG connected with utility grid network.

This remainder of this paper is organized as follows: Chapter II presents the model of photovoltaic DG connected with utility-grid which is studied in this paper and the performance of conventional monitoring parameters including frequency, voltage, ROCOF, power and current. The simulation results show these parameters indeed have large NDZ as described before. Chapter III introduces islanding detection methods based on THD and wavelet transform with their simulation results, respectively. Chapter IV is the newly proposed method and its simulation results analysis. Chapter V presents the final conclusion for this paper.

Chapter 2 Non-detection Zone of Islanding Operation

As what we mentioned in previous chapter, most passive monitoring parameters, such as voltage magnitude, frequency and etc., have large non-detection zone in islanding detection. This chapter mainly discusses this characteristic of current passive islanding methods with several simulation results carried out in a grid connected PV system, introduced in next section.

2.1 Studied Distribution Network

In order to test the performance of the expected islanding detection methods, the author models a distribution network interconnected with a photovoltaic DG in MATLAB/Simulink platform.

Author uses the power distribution network as shown in Fig. 2.1, which consists of single-phase, two-phase and three-phase lateral feeders connected with loads. The detailed parameters of the studied system are given below [22]:

The source is a balanced 60Hz three phase voltage source, with magnitude of 12.47 kV. The source impedances are given in sequence domain as follows:

Positive-sequence: 0.23 + j2.10 ohm.

Zero-sequence: 0.15 + j0.47 ohm.

The feeder impedance matrices in ohms/mile are given as follows.

For the main feeder, the impedance matrix is

[0.3465 + j1.0179 0.1560 + j0.5017 0.1580 + j0.4236

 0.1560 + j0.5017 0.3375 + j1.0478 0.1535 + j0.3849

 0.1580 + j0.4236 0.1535 + j0.3849 0.3414 + j1.0348].

For the three-phase lateral, the impedance matrix is

[0.7526 + j1.1814 0.1580 + j0.4236 0.1560 + j0.5017

0.1580 + j0.4236 0.7475 + j1.1983 0.1535 + j0.3849

0.1560 + j0.5017 0.1535 + j0.3849 0.7436 + j1.2112].

For the two-phase lateral, the impedance matrix is

[1.3294 + j1.3471 0.2066 + j0.4591

0.2066 + j0.4591 1.3238 + j1.3569].

For the single-phase lateral, the impedance is

[1.3292 + j1.3475].

2.2 **Modeling of Photovoltaic DG system**

2.2.1 Inverter classification

Most three-phase DG systems are formed as the scheme like this: a dc source (such as PV array), an inverter (convert DC to AC), a filter (to filter harmonics), a transformer (to step up AC to), and a controller. This scheme is widely used in solar farm systems, fuel cell systems, micro-turbines, and modern wind power systems [20]. Mostly inverter converts the electricity from the DG source to a form that can be used in distribution network (DC to AC). Therefore, the inverters can be classified by the type of distributed generation source. For the source that is driven by a rotating machine at a changing speed such as wind turbines, or engine generators, the output voltage of the variable frequency ac source first need to be rectified to dc and then inverted to a fixed frequency ac that is adapted to the distribution network. For some sources such as photovoltaic DG or fuel cell, the output voltage is a varying dc, thus it need to be stepped up by a dc/dc converter first and then fed into the dc-ac inverter. For some types, the

output dc voltage is also directly connected with a dc-ac inverter [23]. The islanding characteristic of the DG is primarily decided by the type of inverter.

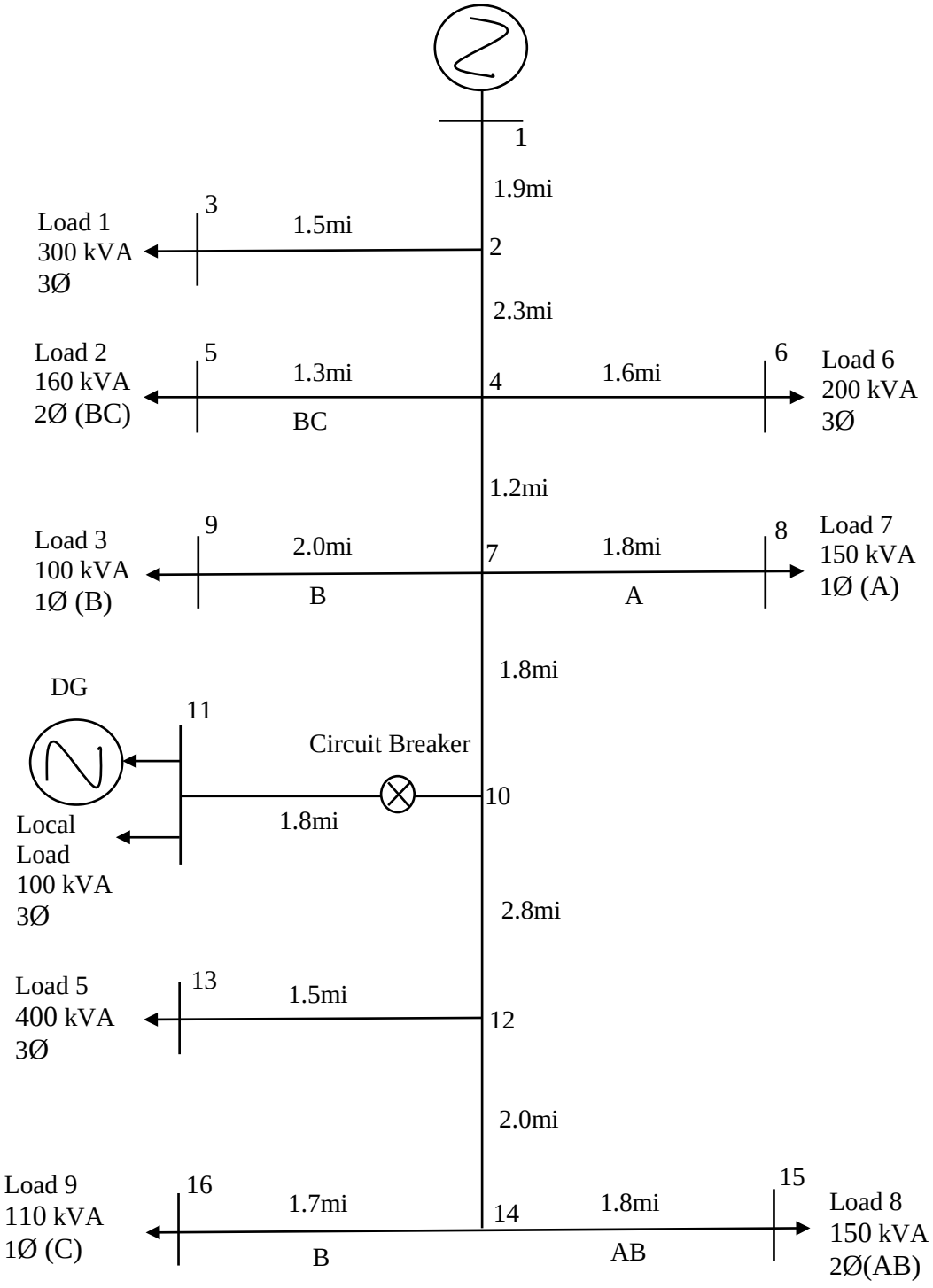

Figure 2.1 Sample Utility Power System Used

2.2.2 Modeling of PV generation

In this paper, author mainly uses the detailed model of a 100-kW grid-connected PV array provided by MATLAB example, which adopts the second type of inverter. The structure of the PV array inverter is shown in Fig. 2.2.

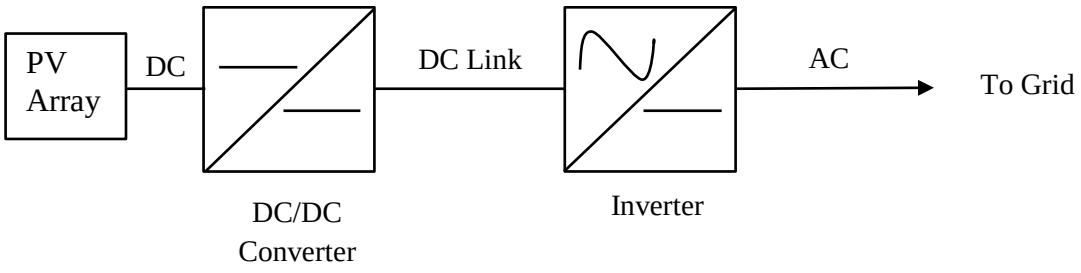

Figure 2.2 Structure of inverter

However, for the detailed structure of DG system, which is shown in Fig. 2.3, we have to take the voltage controller into consideration. From the figure, we can see that a 100-kW PV array is connected to the given 12.47kV distribution network system with a DC-DC boost converter and a three-phase three-level Voltage Source Converter (VSC). Maximum Power Point Tracking (MPPT) [24]is implemented in the boost converter by means of a Simulink model using the Incremental Conductance and Integral Regulator technique.

In Fig. 2.3, the 5kHz DC-DC boost converter increases the voltage from 273 V DC to 500 V DC. In order to improve the efficiency of PV generation, MPPT controller is connected with the boost converter so that the PV array can operate in a maximum power at the expected environmental condition. The 1980-Hz 3 level 3 phase VSC converts the 500 V DC voltage to 260 V AC voltage and keeps the unity power factor. 10

kVar capacitor bank is connected besides the VSC as the filter in order to filter the harmonics produced by the VSC [25].

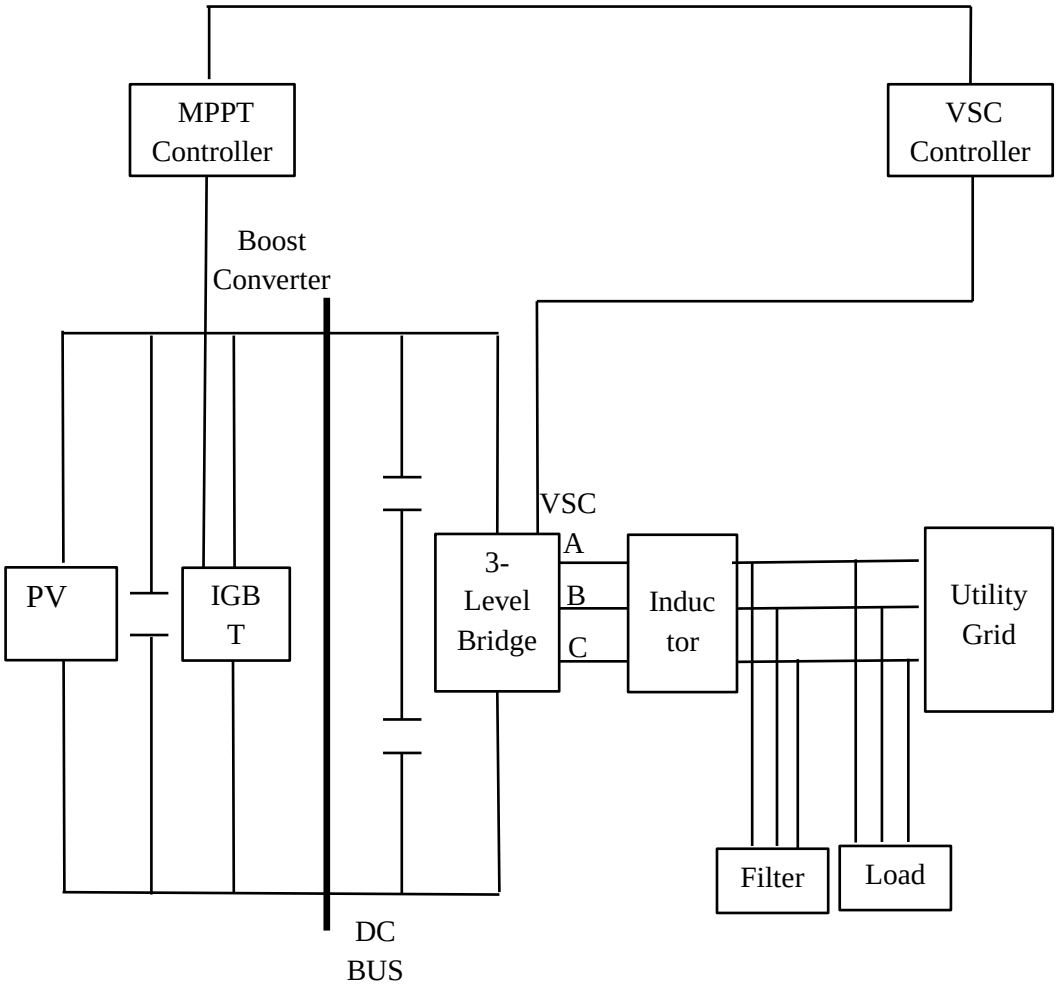

Figure 2.3 Structure of utility grid connected with photovoltaic distributed generator

2.3 **NDZ Characteristics of Islanding Operation**

In this section, author first tests several monitoring parameters such as voltage magnitude (pu), current (pu), frequency (f), power (P) and rate of change of frequency (df/dt) at the end of DG or the Point of Common Coupling (PCC). In order to simulate the situation of islanding, the distribution network processes in the mechanism shown in

Fig. 2.3. We assume the islanding operation of DG will happen after loss of main source power. The circuit breaker will be open at t=0.2s to model islanding. Generally, the system will be operated under two typical cases of islanding condition: large power mismatch and small power mismatch for the DG rated power with the local load power. In math, the power mismatch can be defined as [26]:

$$\Delta P = \frac{P_{load} - P_{inv}}{P_{inv}} \times 100\%$$

$$\Delta Q = \frac{Q_{load} - Q_{inv}}{Q_{inv}} \times 100\% \quad (2.1)$$

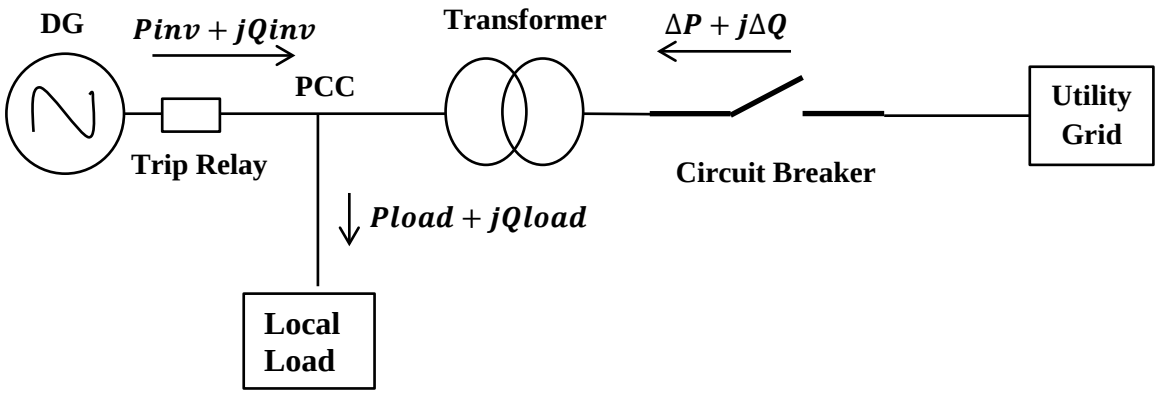

Figure 2.4 Mechanism of Islanding Operation

The behavior of the system after islanding is based on ΔP and ΔQ when the DG is disconnected from utility grid. If $\Delta P \neq 0$, the output voltage magnitude at the PCC end will change, then UVP/OVP relay can detect this variation and send a trip signal.
If $\Delta Q \neq 0$, OFP/UFP can detect the variation of system frequency caused by sudden change of load voltage.

However, this method may not detect islanding if the local load power is close to the DG nominal power, the voltage and frequency variations may not be enough to reach

the voltage and frequency preset threshold. In addition, the threshold is usually extremely wide so that the inverter can adapt to the normal variations in grid voltage and frequency without disconnection. This limit causes the phenomenon what we have mentioned before - large non-detection zone of voltage and frequency islanding detection. This is the major drawback of the methods which rely on voltage magnitude and frequency measurement. Actually, this phenomenon has been fully documented in many papers. When some similar conditions happen, the PV inverter may fails to detect the disconnection of utility and keep on operating, then causing islanding. Some conclusions about the NDZ have been verified [27] [28] [29]:

When ΔP is large: The voltage at the DG end will vary remarkably and the magnitude will reach the threshold setting easily. Normally islanding condition can be detected accurately if $\Delta P > \pm 20\%$.

When ΔP is small but ΔQ is large: Output frequency will vary dramatically and the frequency rises above the limits. The islanding detection scheme may fail to detect when the load condition setting is $\Delta P = 0$, and $\Delta Q < \pm 5\%$.

When ΔP&ΔQ are small: if power setting is $\Delta P < \pm 20\%$ and $\Delta Q < \pm 5\%$ then voltage magnitude and frequency variations may be too small to detect islanding.

Other normal monitoring parameters also show this limitation and have low islanding detection accuracy. Next section discusses the NDZ character of islanding detection with the two cases in detail, respectively.

2.3.1 Large Power Mismatch after Islanding

For the first case (large power mismatch), islanding is easily to be detected based on the conventional parameters because the sudden large changes of the DG load, there

will be large variations in the voltage magnitude, frequency, ROCOF and current. Here we set the power mismatch equals 50% ($\Delta P = -50\%$), which means the local load power in this case is 50 kW and the nominal power supplied by the PV inverter is 100 kW. For simplicity, only the simulation results of Phase A have been shown in Fig. 2.4(a)-(d). From the results, we can see the large load variation causes the voltage at the end of the inverter greatly rises above the preset voltage magnitude range ($V_{max} = 110\%, and\ V_{min} = 88\%$) as shown in Fig. 2.4(a). Fig. 2.4 (b) also shows the system frequency measured at the PCC by using phase-locked loop (PLL) is out of the setting threshold (59.3 – 60.5 Hz), which is required by the Standard 1574. The variations of current magnitude and ROCOF are also dramatic shown in (c)-(d). Therefore, conventional passive islanding detection methods are available and effective under large power mismatch.

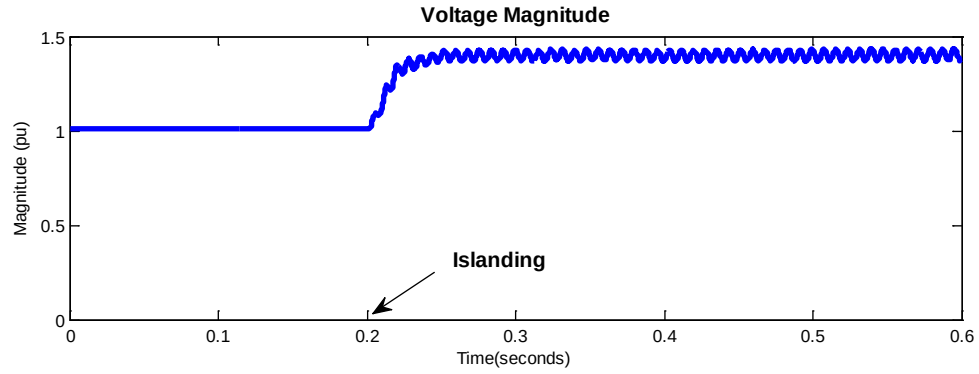

(a)

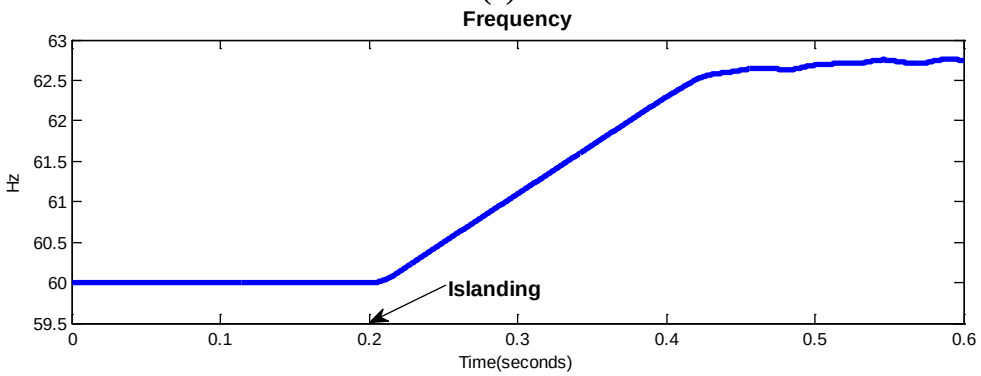

(b)

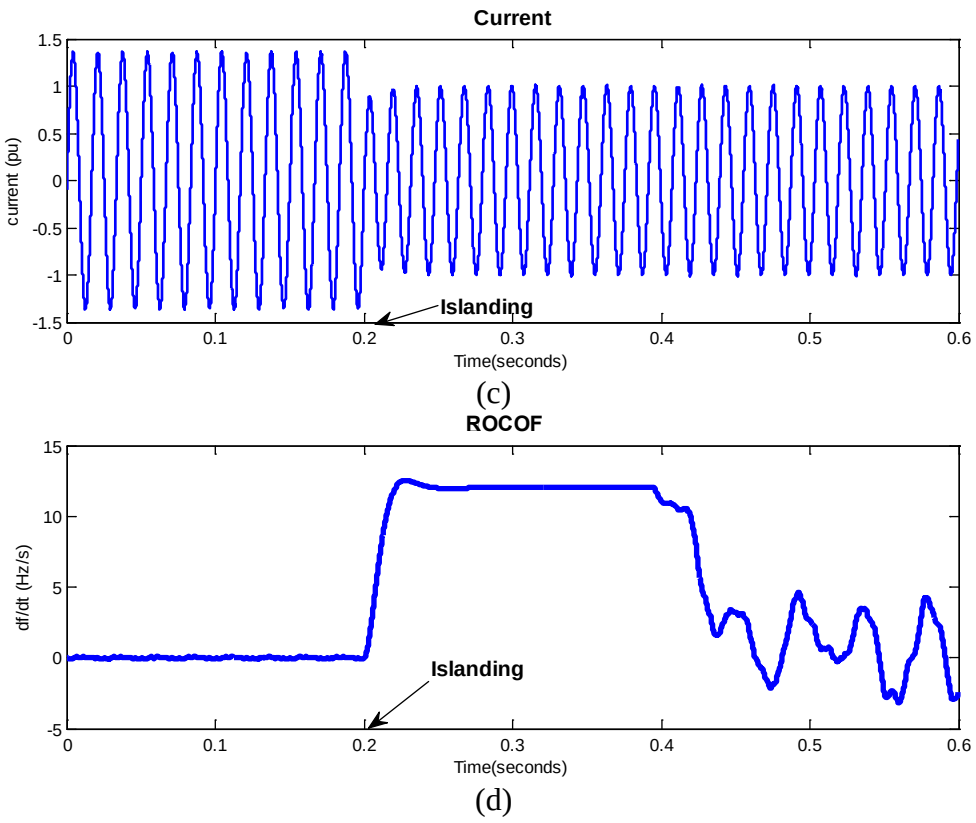

Figure 2.5 Parameters for large power mismatch after islanding. (a) Voltage Magnitude of Phase A. (b) Frequency (c) Instantaneous Current of Phase A (d) ROCOF.

2.3.2 Small Power Mismatch after Islanding

For the second case (small power mismatch), in order to best examine the assumption, we set the worst islanding condition, power mismatch equals zero ($\Delta P = 0\%$). Because the PV inverter keeps the unity power factor, so we set the load power $P_{Load} = P_{PV} = 100kW$. The result has been shown in Fig. 2.5(a)-(d). As we expected, under this small power mismatch condition, the voltage and frequency at the end of PV inverter after islanding (0.2s) keep the same with the situation when utility grid was connected. Thus, the result confirms that the conventional passive methods fail to detect the islanding operation in small power mismatch because the monitoring parameters do

not change enough under the threshold setting proposed by IEEE 1574 (shown in Table 1.1 and 1.2).

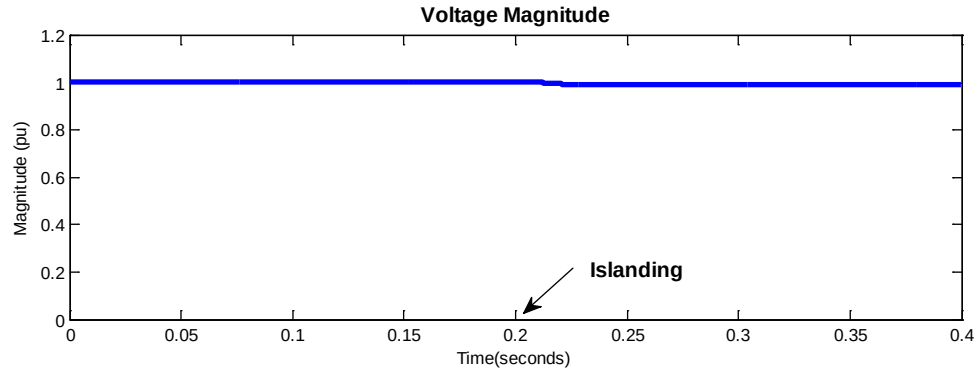

(a)

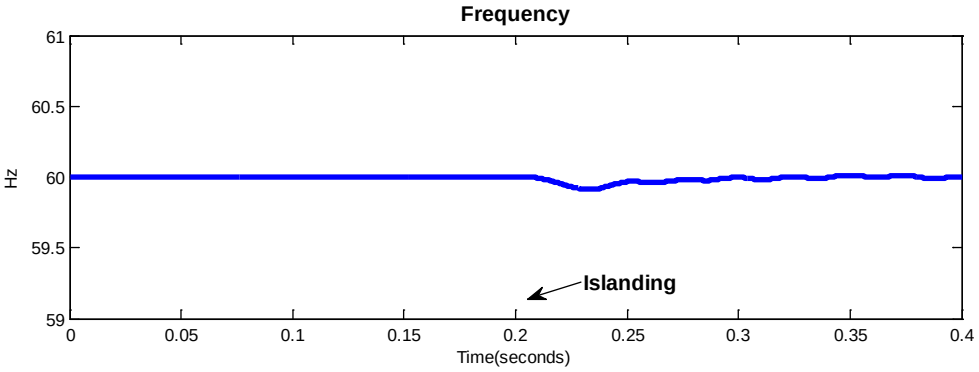

(b)

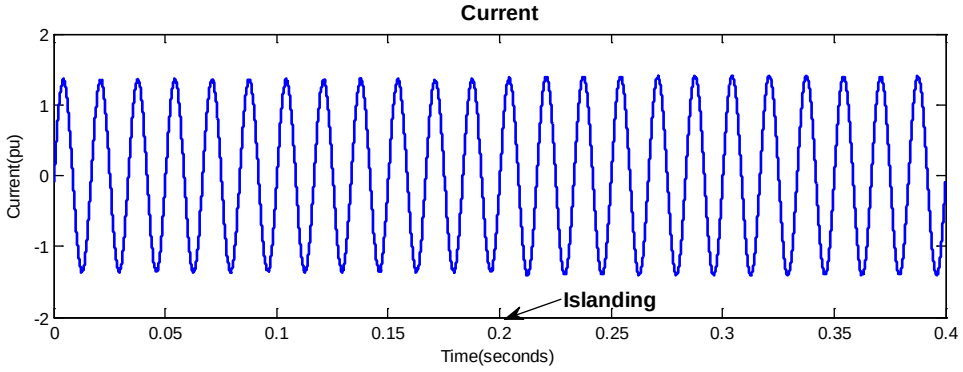

(c)

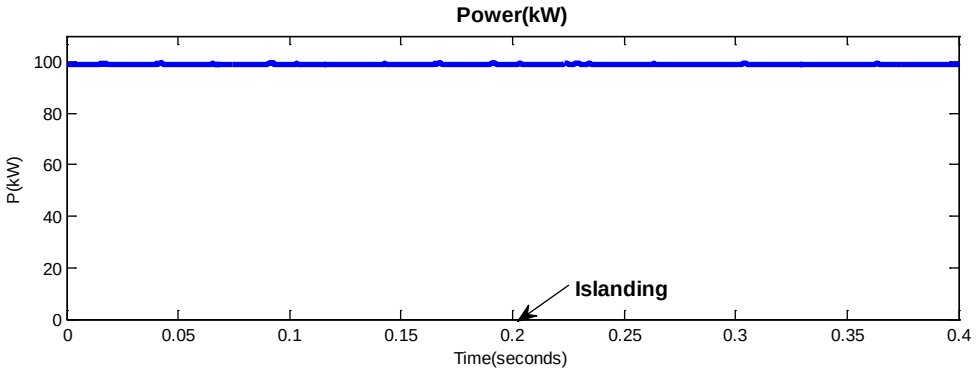

(d)

Figure 2.6 Parameters for small power mismatch after islanding. (a) Voltage Magnitude of Phase A. (b) Frequency (c) Instantaneous Current of Phase A (d) Power at PCC.

However, for this system, the area of NDZ is much larger than 20%. The simulation results (Fig. 2.6a) show the frequency reaches the threshold limit when we set power mismatch equals 28.7% ($\Delta P = -28.7\%, P_{Load} = 71.3kW, P_{PV} = 100kW$). That means if the power mismatch is less than 28.7%, the conventional monitoring parameters will fail to detect islanding. Similarly, when$\Delta P = -13\%, P_{Load} = 87kW, P_{PV} = 100kW$, the voltage magnitude method fails to detect islanding, shown in Fig. 2.6b. We also can find the upper limit of NDZ for frequency and voltage magnitude method, respectively.

For frequency:

$$-28.7\% < \Delta P < 50\%$$

For voltage magnitude:

$$-13\% < \Delta P < 32\%$$

Therefore, it is highly necessary to find another effective way to decrease the area of NDZ. Next section will mainly introduce THD and voltage unbalance method which may solve this problem.

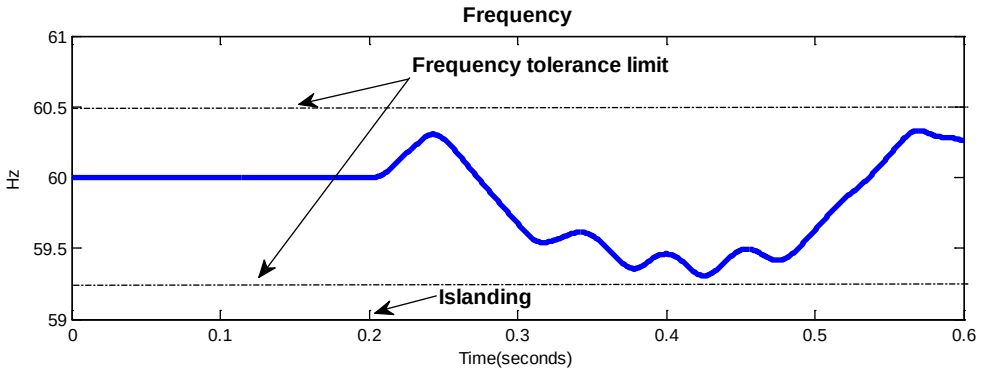

(a)

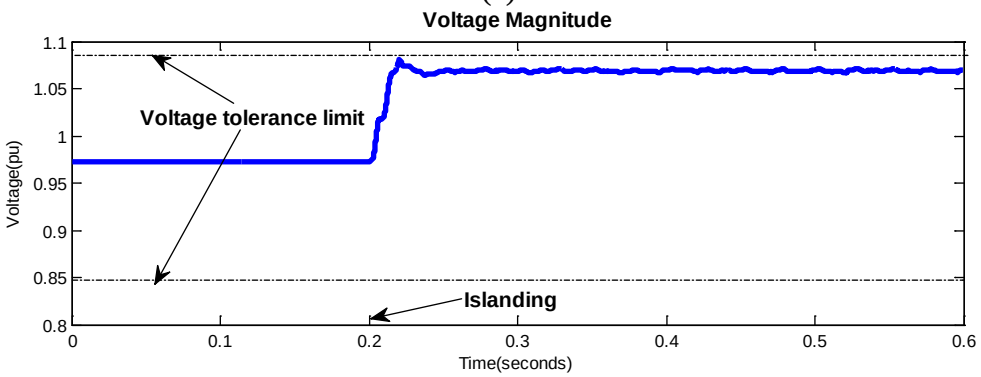

(b)

Figure 2.7 Passive methods fail to detect islanding (a) after $\Delta P < 28.7\%$ by monitoring frequency. (b) after $\Delta P < 13\%$ by monitoring voltage magnitude.

Chapter 3 Islanding Detection Using THD VU and Wavelet-Transform

Since the conventional monitoring parameters are not good enough to detect the islanding under small changes in the loading of DG after islanding, author finds other two ways for islanding operation of DG: 1) by monitoring voltage unbalance and total harmonic distortion (THD) of voltage. 2) Wavelet-Transform.

3.1 Islanding Detection Using Voltage Unbalance and Total Harmonic Distortion

3.1.1 Definition of THD and VU

1. Voltage Unbalance Variation

Even though the load for the DG does not change too much after loss of main source, the topological structure the DG network has been changed. As we known, negative sequence component of three-phase voltage is widely used to detect fault and unbalanced conditions in transmission system. So we can imagine the voltage unbalance factor, which is based on negative and positive sequence voltage components of the three-phase output voltage of the DG, may be an effective parameter to monitor the occurrence of islanding. First, we need to define the voltage unbalance factor.
The exact definition of voltage unbalance is defined as the ratio of negative sequence voltage component to the positive sequence voltage component. The percentage unbalance factor (VUF), is given by [30]:

$$VUF = \frac{Negative\ sequence\ voltage\ component}{Positive\ sequence\ voltage\ component} \times 100 \qquad (3.1)$$

2. THD Variation of voltage at the end of DG

The total harmonic distortion, or THD of a signal is an important parameter to evaluate the power quality of electric power systems. Similarly, with the changing topological structure of the loading of DG, the THD of the voltage at the end of inverter may also be changing dramatically since it is more sensitive than other monitoring parameters. The mechanism is that, in normal operation, the distribution network works like a stable voltage source, powering the inverter terminal with a low voltage distortion. However, after islanding is formed, the voltage THD may increase because the output circuit impedance at the DG end increases because the distribution network which has low impedance is disconnected with the DG system and DG keeps powering the remaining local load alone. Thus, current harmonics will cause increasing levels of voltage harmonics at the DG end.

So we propose the THD of the voltage as another indicator of the happening of islanding. THD of the voltage at the monitoring time t can be defined as [31]:

$$THD_t = \frac{\sqrt{V_2^2+V_3^2+V_4^2+\cdots+V_n^2+\cdots}}{V_1} \times 100 \qquad (3.2)$$

Where V_n is the RMS voltage of nth harmonic and V_1 is the rms value of fundamental component. For a pure sinusoidal voltage, the THD has a null value.

3.1.2 Studied method

Each of the two monitoring parameters described above can be used to detect islanding successfully if we choose appropriate threshold limit. However, it is extremely hard to set an appropriate threshold limit for the system to make sure any of these methods would be able to detect islanding without mal-operation for non-islanding situation. This is because if too many disturbances are introduced to the system,

especially for adding some non-linear load such as diode devices and MOSFET, or introducing pulse signal, the THD and VU variations may also reach the tolerance limit causing a mal-operation of trip relay.

However, we can effectively avoid mal-operation with the method if we make a small change with the threshold setting method. It can be easily imagine that the topological structure of the DG network has been largely changed since the DG has to power the local load by itself after loss the main power of utility grid. Thus, the steady-state of the DG network mainly has been also changed after islanding. This is the major difference between islanding and non-islanding condition. Thus, based on this difference, a new criterion is proposed in [20].

First, we define the voltage unbalance and THD variations as follows, which measure the deviation of VU and THD from steady state and normal loading condition:

$$\Delta THD = \frac{THD_{stable} - THD_S}{THD_S} \times 100\%$$

$$\Delta VU = \frac{VU_{stable} - VU_S}{VU_S} \times 100\% \quad (3.3)$$

Where VU_s,THD_s is the initial set for the steady-state before islanding, and $THD_{stable}, VU_{stable}$ is the stable value right after three power cycles after events introduced (including islanding and non-islanding) to avoid the transient period. Then the rule of islanding is proposed as follows:

$$\Delta THD > 75\% \; or \; \Delta THD < -100\%$$

$$\Delta VU > 50\% \; or \; \Delta VU < -100\% \quad (3.4)$$

If the monitoring parameters satisfy the above criterion, we treat it as occurrence of islanding and make a trip signal.

3.1.3 Test results

Case 1: Islanding operation at DG end

In order to test the performance the studied method, author first simulates the islanding operation condition of DG with the network proposed. In this case, author calculates the changes of voltage unbalance and THD of voltage under the small power mismatch condition ($\Delta P = -10\%, P_{Load} = 90\ kW,\ P_{PV} = 100\ kW$). Islanding operation is also modeled by opening the circuit breaker at the end of DG. As we expected, the simulation results of conventional monitoring parameters (voltage magnitude of PCC voltage phase A and corresponding frequency), shown in Fig. 3.1 (a)-(b), obviously do not change enough to detect the islanding operation. However, unlike other parameters, the voltage unbalance factor and THD of voltage change largely due to the sudden change of DG network after islanding (Fig. 3.1(c)-(d)), and the resulted THD stable error $\Delta THD = 513\%$, which satisfies the rule (3.4) and this case can be decided as islanding. This result shows that this method outperforms the conventional monitoring parameters, which have difficulties to detect the islanding with small power mismatch. So it is reasonable to set the large change of VU and THD as a signal of occurrence of islanding operation.

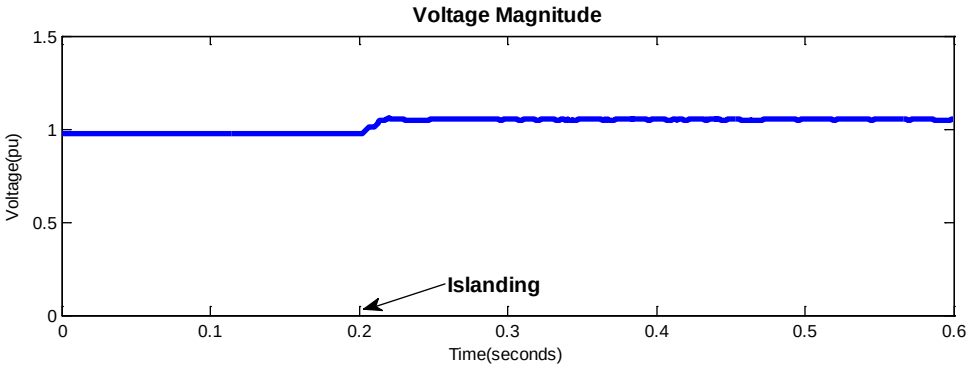

(a)

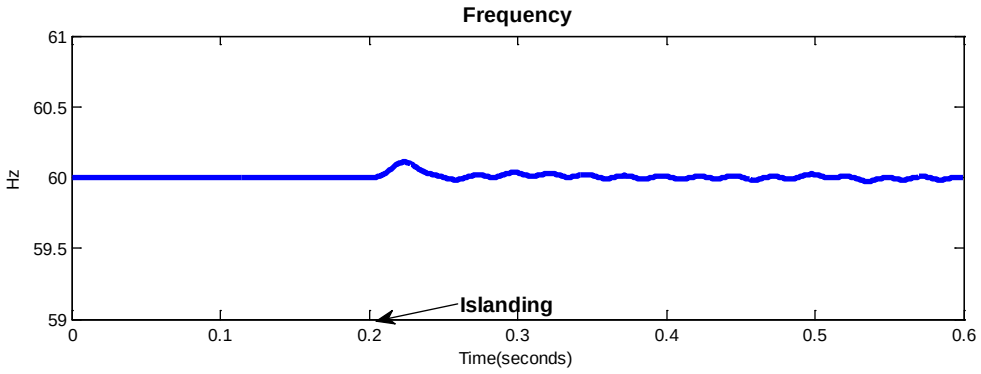

(b)

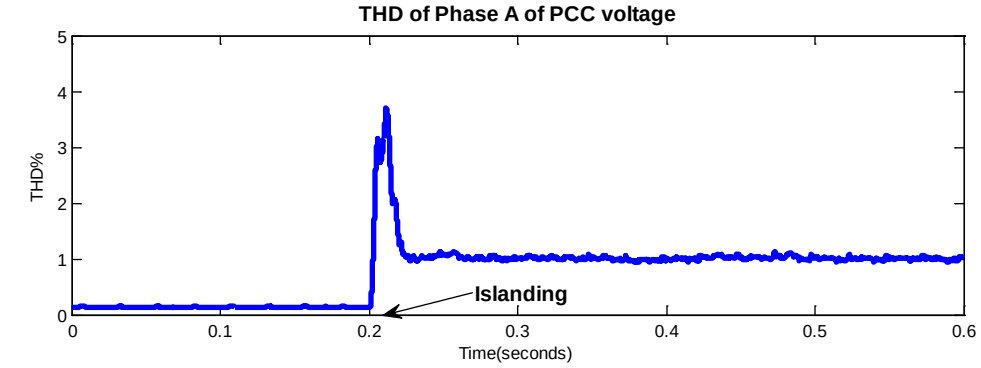

(c)

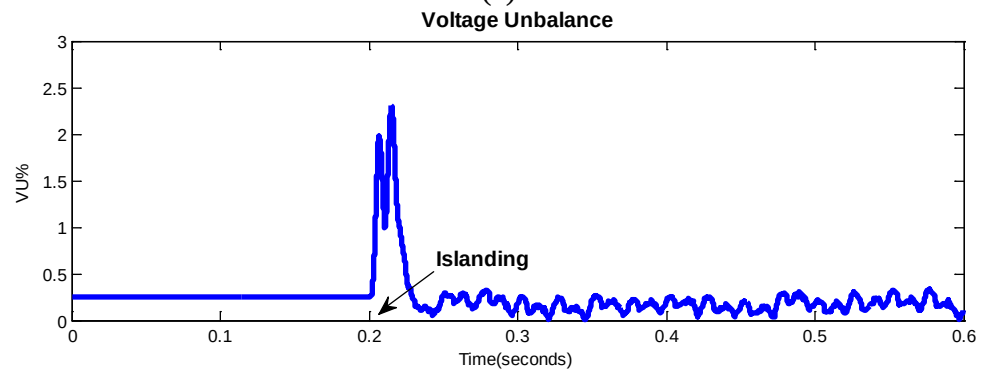

(d)

Figure 3.1 Small power mismatch with different monitoring parameters. (a) Voltage magnitude. (b) Frequency. (c) THD of phase A voltage. (d) Voltage unbalance.

Several test results of proposed monitoring parameters with some normal non-islanding disturbance, including fault, pulse noise, are presented in this section in order to distinguish islanding with non-islanding condition. Due to the change of network structure, these cases may also show similar results with islanding, confusing the

operation of trip relay. Therefore, it is meaningful to study normal load variation comparing with islanding.

Case 2: Fault happens at utility grid

Due to lightning or storms, single line to ground fault often occurs in power system. Therefore, for this case, author introduces a single line to ground fault at Phase A in Bus 12 (fault impedance$Z_F = 35\Omega$), then the circuit breaker will open after three power cycles in order to clear the fault. That means the utility grid will lose the branch of load 5. However, in this case all the phases need to be monitored because unbalanced fault may cause different results for different phases. This is quite different with islanding because all the three phases have been tripped after islanding. The following figures show the corresponding test results of the case.

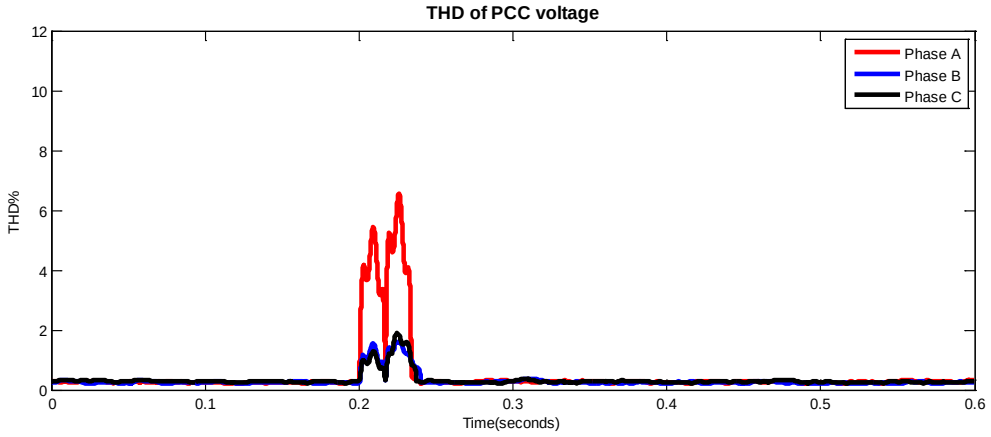

(a)

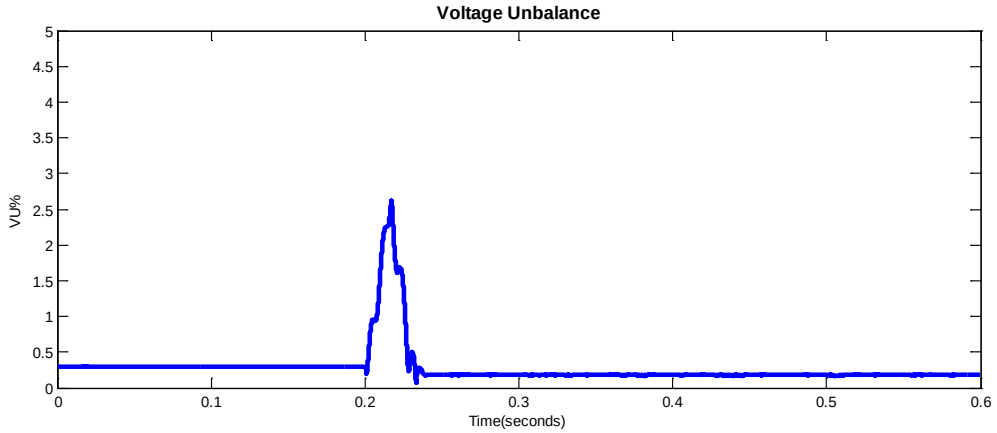

(b)

Figure 3.2 Test results of Case 1 (a) THD of PCC voltage. (b)Voltage Unbalance

From the figures, we can easily find VU and THD parameters vary very remarkably. All the THD values of three phases have reached the maximum value at 0.23s. Then if we keep monitoring the parameters for one more power cycle, when the fault is clear, we find all of them drop down to the almost same stable value level with the state before fault occurrence, which means $\Delta THD = 5.3\% < 75\%,\ \Delta VU = -38\% > -100\%$. This is because when the circuit breaker is open to clear the fault, only load 3 is lost from the network. Thus the topological structure of remaining network won't cause the change of steady-state as much as islanding did. So we can easily distinguish single line to ground fault with islanding based on the stable error criterion (3.4) and the trip relay will not mal-operate.

Case 3: Pulse disturbance happens at utility grid

In real power system, a fast short duration electrical transients called voltage spikes always happen to damage power supply because of lightning strikes, power outages or short circuits. So in the third case, author introduces a single phase pulse disturbance (clear in a short time) at 200ms in Bus 7 phase A, shown in Fig. 3.3, to model this situation.

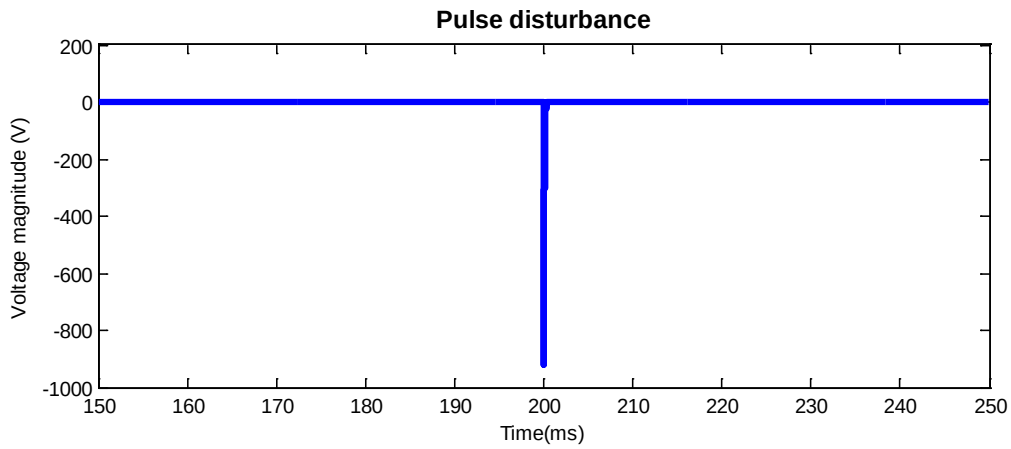

Figure 3.3 Pulse disturbance in power system

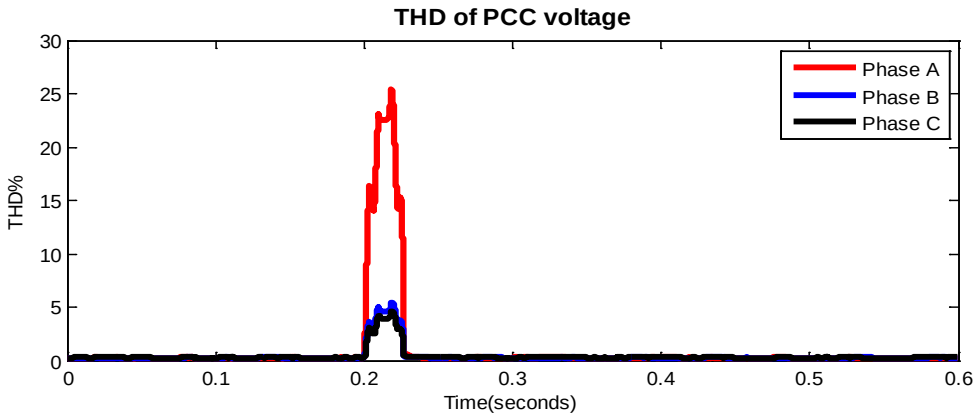

(a)

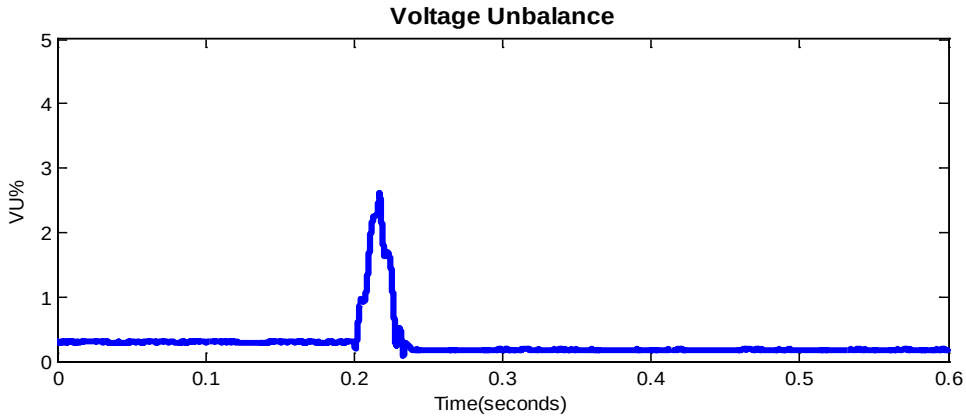

(b)

Figure 3.4 Tests results of Case 2 (a) THD of PCC voltage. (b) Voltage Unbalance.

The simulation results (Fig. 3.4) show similar behaviors with islanding because the three monitoring parameters varies dramatically, but the steady-state does not change

as much as islanding did, $\Delta THD = 1.5\% < 75\%,\ \Delta VU = 1\% < 50\%$. Thus the trip relay won't mal-operate according to criterion (3.4). This phenomenon is similar with the test results of case 2.

Although the THD&VU method works well in these three typical cases, there are still some problems when we use the method in this case. First, in islanding case, even though the voltage unbalance factor changes abruptly, it is hard to find a steady-state to decide the stable value of VU due to the unstable system after islanding. That means this method may fail to detect because of the long oscillation period. What's more, the setting of VU threshold is questionable because some normal load variation also can cause the VU factor exceed the threshold and make a wrong decision. Second, in [20], the THD parameter is calculated with the ideal voltage signal waveform, but in practice, voltage signal is always mixed with noise caused by devices which produce quick spikes in voltage or current, such as switching-on large electrical motors, lightning strike, high-voltage surge and etc. Therefore, although THD&VU method works well in [20], it may show unexpected result if we introduce some noise disturbance into the original voltage waveform. Next two cases show the studied method fail to detect or mal-operate to some non-islanding condition.

Case 4: Islanding detection with distorted voltage signal

In this case, author tries to analyze the influence of noise disturbance on THD islanding detection. In order to compare with case 1, author also sets the same power mismatch $\Delta P = -10\%$, but introducing some white noise into original voltage waveform. Fig. 3.5 shows a typical voltage waveform superimposed with noise.

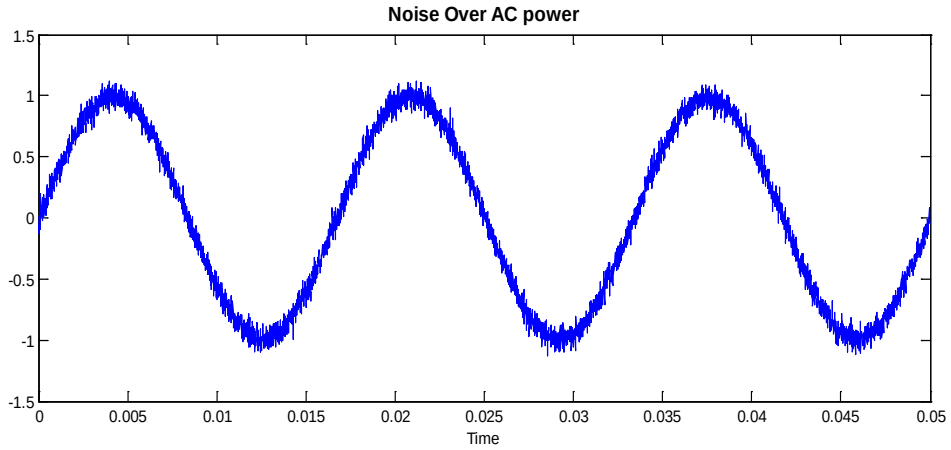

Figure 3.5 Voltage signal mixed with noise

The simulation result (Fig. 3.6) shows the THD does not change too much after islanding and the resulted $\Delta THD = 7\% \ll 100\%$. This result is quite different with the situation before noise introducing. Thus, this method fails to detect islanding with practical signal or at least it has a much larger NDZ than what [20] said.

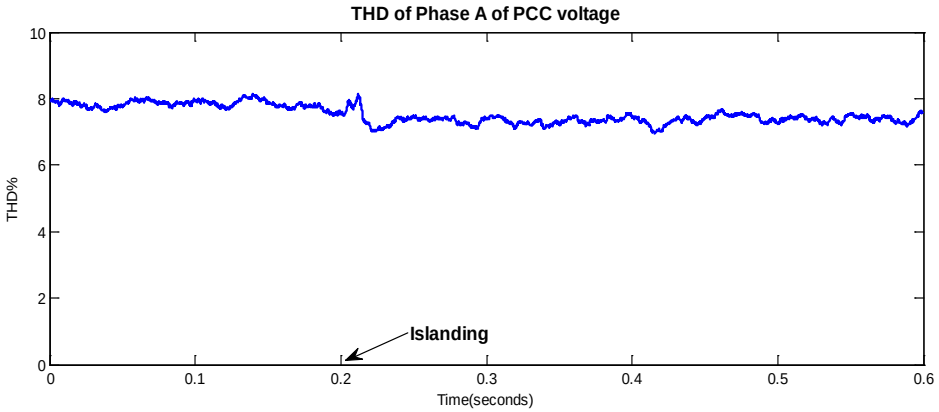

Figure 3.6 THD analysis with noise disturbance

Case 5: Disconnection of a branch of load

In this case, a circuit breaker is installed between Bus 10 and Bus 12 and will be disconnected at t=0.2s so that the utility grid will lose the load under Bus 12. The VU result has been shown in Fig. 3.7.

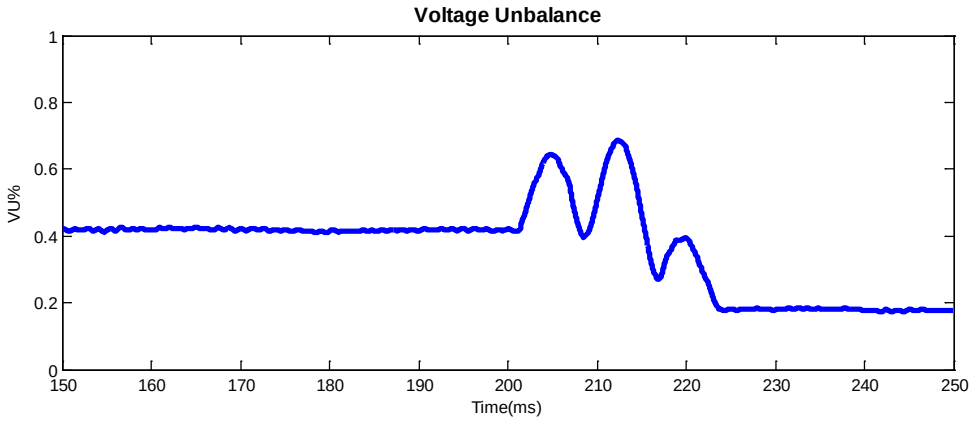

Figure 3.7 Voltage Unbalance for Case 5

From the figure, we can easily see although this case is a non-islanding event, the voltage unbalance also shows large change after losing the branch of load. The stable error $\Delta VU = 58\%$ is even beyond the 50% threshold setting. Therefore, in this case, the studied method may treat it as an islanding event and make a wrong decision.

3.1.4 Conclusion

Even if the corrected THD&VU method has better performance than other conventional islanding detection, the simulation results at least demonstrate two problems of this method: 1) It is still based on the threshold setting thus it has NDZ. 2) De-noising is very important dealing with practical voltage signal. In order to solve these problems, author found another method proposed in [20] which is based on wavelet-transform to see if it has better performance.

3.2 Wavelet-based Islanding Detection Method

Actually, wavelet theory has been widely used in power system, like feature extraction, de-noising and data compression of power quality waveforms, power system protection etc. [32] [33] [34]. In power system, transient waveforms of currents and voltages are very important for fault analysis because they may contain useful

information demonstrating the reason why the transient event occurs. In other words, the transient state of utility voltage and current has some high frequency components that are not detectable by conventional methods on a power frequency. Hence in order to distinguish islanding from other normal load operation, it is very necessary to perform wavelet analysis on the original current or voltage waveforms to extract a useful feature to achieve the classification [35]. So it is reasonable to imagine wavelet transform can solve the drawbacks of the methods we have studied to some extent and to be an effective tool to detect islanding.

3.2.1 Brief Introduction to Wavelet Transform

In this section, only a brief explanation of wavelet theory related to islanding detection is presented.

Wavelets are functions, used to efficiently describe a signal by decomposing it into its constituents at different frequency bands (or scales), which are known as wavelet coefficients [36]. By passing through a low pass filter with impulse response$g$, the first level of DWT of objective signal $x(n)$ is calculated, resulting giving the approximation coefficients ($a_1(n)$), and passing through a high pass filter$h$, resulting giving the detail coefficients ($d_2(n)$). The filter outputs are then subsampled by 2. Then this process can be repeated to decompose more levels of the approximation coefficients with high and low pass filters and then subsampled by 2 as similar. This process has been shown in Fig. 3.8 - Fig. 3.9 [37]. The equations below explain the calculation of approximation coefficients and detail coefficients [21].

$$a_m(n) = \sum_n g(2n-k)a_{m-1}(k)$$

$$d_m(n) = \sum_n h(2n-k)d_{m-1}(k) \tag{3.5}$$

Where $a_m(n)$ represents the approximation coefficients at level m, wavelet coefficients (detail coefficients) $d_m(n)$, represents signal detail at level m.

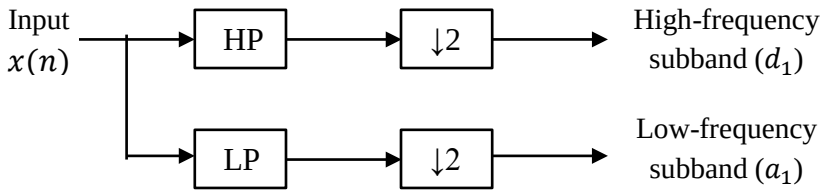

Figure 3.8 Structure of wavelet filter bank analysis

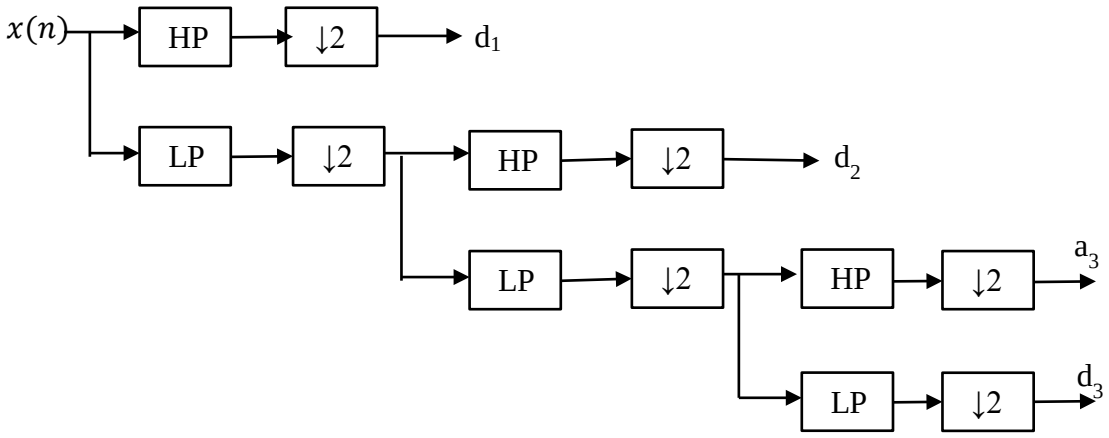

Figure 3.9 3-level DWT decomposition

Mathematically, discrete wavelet transform (DWT) of a discrete signal $f(k)$ is defined as [37] [38] [39]:

$$DWT_{\varphi} f(m,n) = \sum_k f(k)\varphi^*_{m,n}(k) \tag{3.6}$$

Where $\varphi_{m,n}$ is the discretized mother wavelet given by

$$\varphi_{m,n}(t) = \frac{1}{\sqrt{a_0^m}}\varphi\left(\frac{t - nb_0a_0^m}{a_0^m}\right)0 \tag{3.7}$$

Where, $a_0(>1)$ and $b_0(>1)$ are fixed real values, and m and n are positive integers. In this paper, Daubechies wavelet transform with 5 levels is used to deal with the transient signals.

Compared with the conventional monitoring parameters, which may fail to detect the islanding operation under small power mismatch because the parameters are still within the threshold setting, wavelet method is much easier to react to the spectral changes occurring at higher frequency components of PCC voltage caused by islanding so that detect the islanding with a smaller NDZ and even without injecting any signals to influence the power quality. In the studied method, the three-phase voltage at the end of PCC is decomposed to a chosen level by DWT which is introduced in the previous section.

Firstly, we only considerV_a , the voltage of Phase A (RMS value), and $[d_1, d_2, \dots\dots, d_5]$ as resulting outputs of 5 levels DWT decomposition, where d_m represents the wavelet coefficients at the Level m frequency wavelet band. As for the mother wavelet, “db1” has been used due to its compactness, and localization properties. Fig. 4.4 shows the initial study for the “close to zero” power mismatch case.

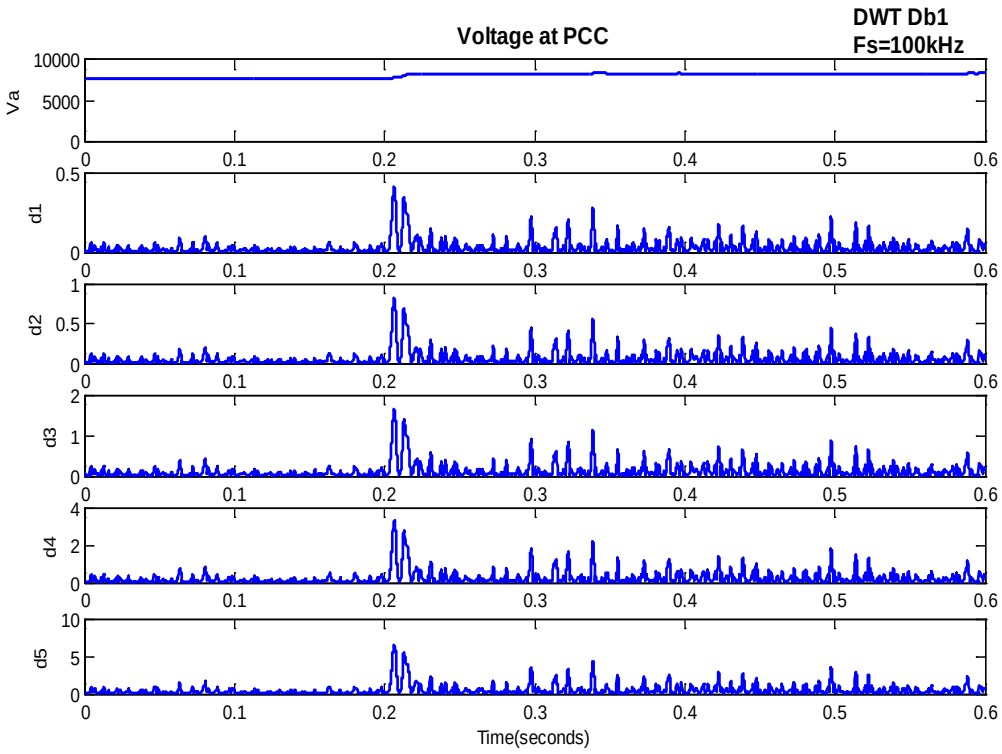

Figure 3.10 Five level DWT decomposition of V_a

As shown in Fig. 3.10, the wavelet coefficients show large changes after islanding. Thus we can imagine proposed method can be used as an effective tool for islanding detection if we choose appropriate threshold setting for wavelet coefficients. But as what we did before, we still need to take the normal load variation operations into consideration because these operations may also produce high magnitude wavelet coefficients so that it may cause nuisance tripping. Therefore, only based on the threshold setting of wavelet coefficients magnitude may be not enough for islanding detection. Thus, a new concept – energy of the wavelet coefficients, is proposed. The energy content for three-phase PCC voltage is defined as [21]:

$$E_j = \sqrt{\left[\sum_{i=1}^{i=N} \frac{abs^2\left(d_{jm}(i)\right)}{N}\right]} \tag{3.7}$$

Where, $j \in \{a, b, c\}$, represents the three phases and N is the number of coefficients for every power cycle.

3.2.2 Studied Method

In [21], the author used magnitude of wavelet coefficients (abs value) and energy content as the threshold setting for islanding. Therefore, author tries to simulate several islanding or non-islanding conditions to study whether there is a hidden regularity in wavelet coefficients and energy content magnitude to distinguish different situations.

3.2.3 Test Results

To test the performance of the new wavelet-transform based method, author also simulates the photovoltaic DG network connected with utility grid system in MATLAB as what we did before. A various of islanding and non-islanding cases are tested.

Case1: Islanding operation

Different islanding situations (large power mismatch and small power mismatch) have been created by changing its power demand of local load connected with DG. Since large power mismatch case can be easily detected by other methods, for brevity, only the small power mismatch case ($\Delta P = 15\%, P_{Load} = 115kW, P_{PV} = 100kW$) is shown in this paper. For case study the islanding is created at 0.2s by opening the breaker circuit as similar with the previous tests. In this test, the ‘db1’ mother wavelet has been chosen and the fifth level of wavelet transform has been used to analyze due to its robustness and least affected by the noise. From the results (Fig. 3.11), it can be easily seen both Phase A and Phase B voltage at the end of DG not changing too much (still remain within the operating range) after islanding thus demonstrating the passive method based on OUP/UUP relays fails to detect islanding. However, the absolute value of wavelet

coefficients and corresponding energy values calculated by equation (3.7) show large change after islanding.

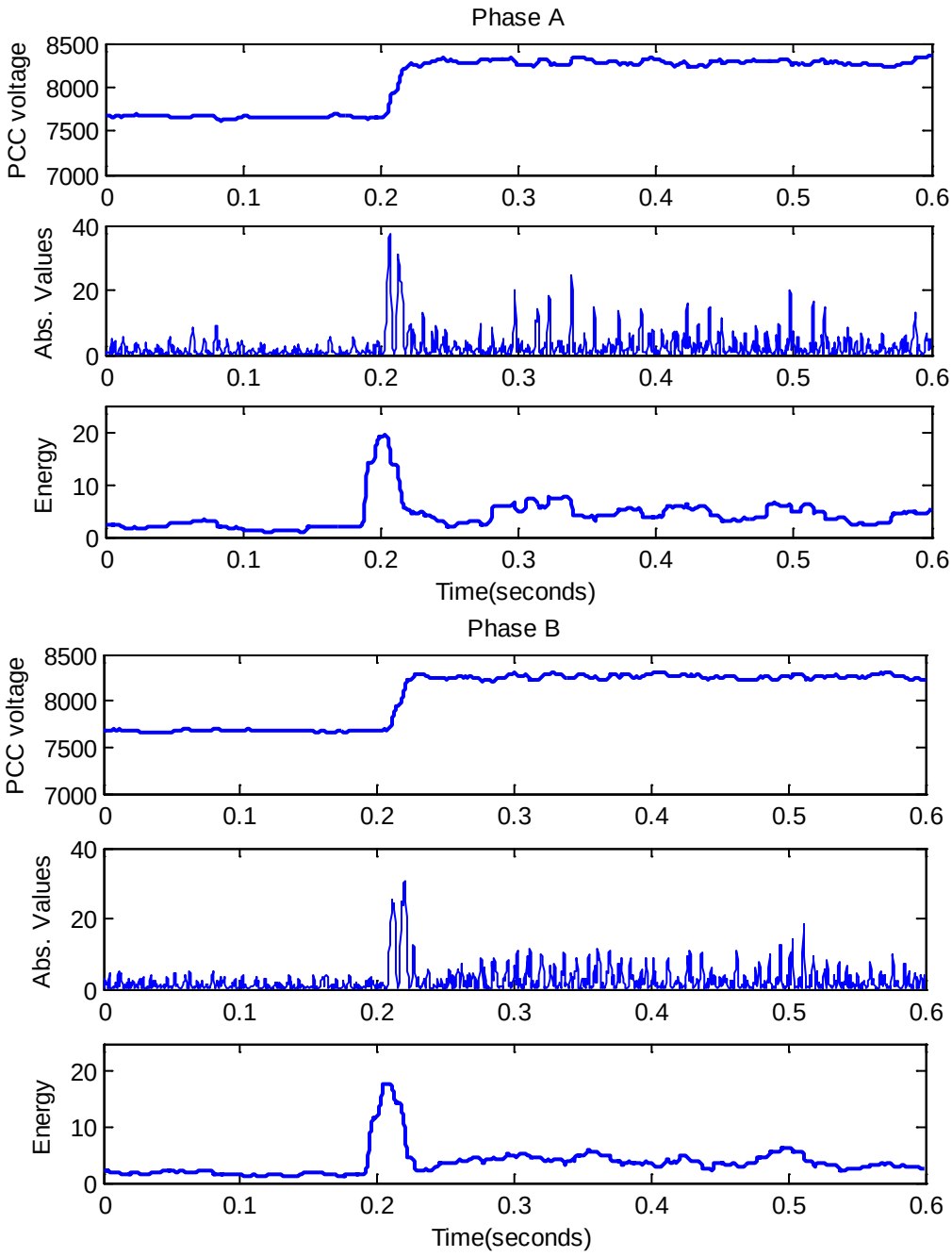

Figure 3.11 Wavelet analysis for islanding

As similar with previous chapter, normal fault disturbance cases were carried out to test its selectivity. The considered events are same with THD method studied before.

Case2: Single line to ground fault happens at utility grid

In this case, author set a single line to ground fault at Bus 10 Phase a (t=0.2s). Fig. 3.12 shows the corresponding simulation results.

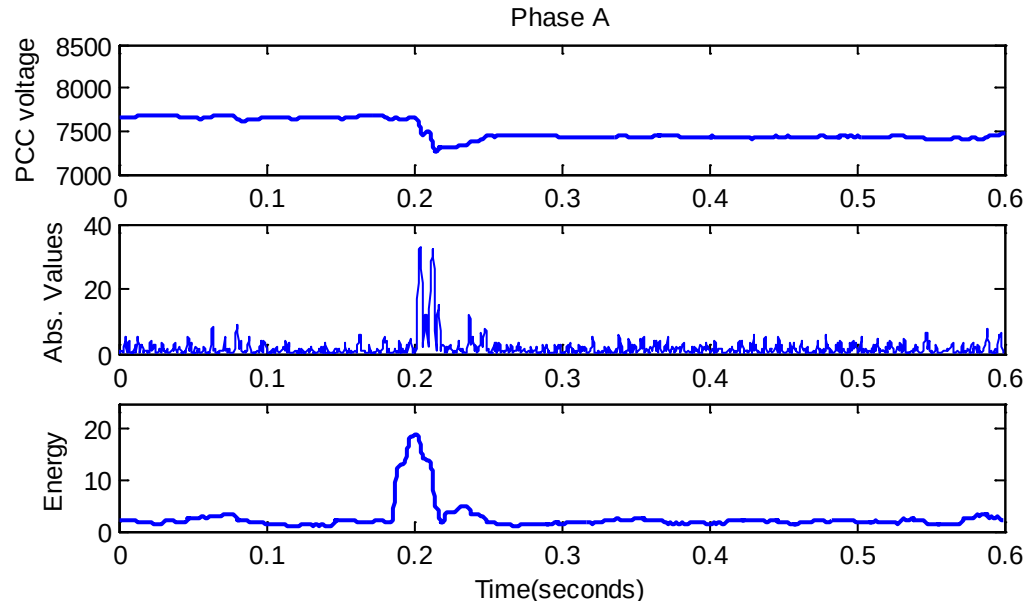

(a)

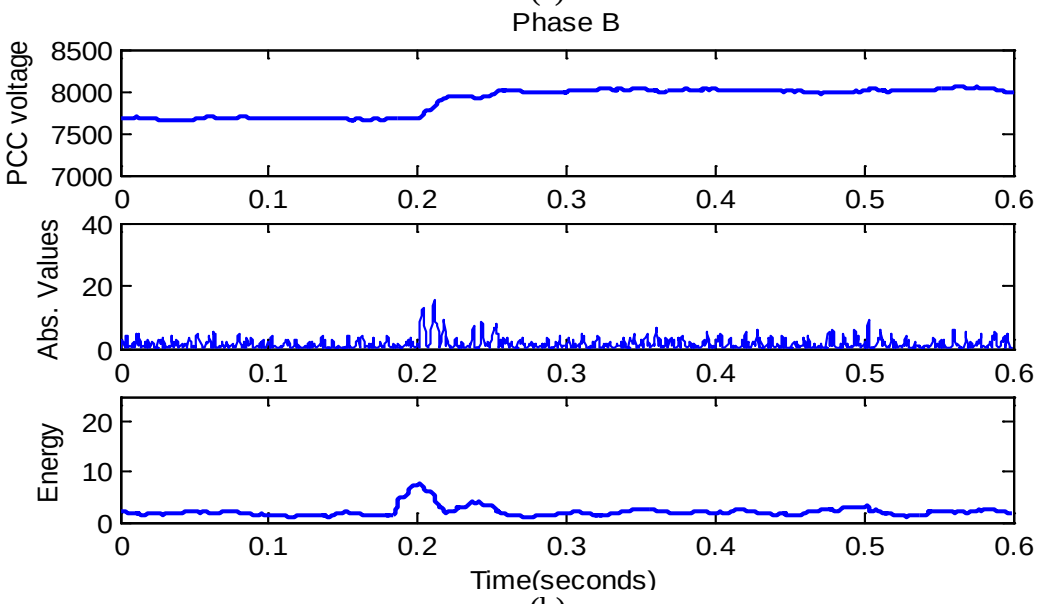

(b)

Figure 3.12 Wavelet analysis for Case 2

Case 3: Pulse disturbance introduced

In this case, pulse disturbance was introduced into main distribution network. Figure 3.13 shows the corresponding results.

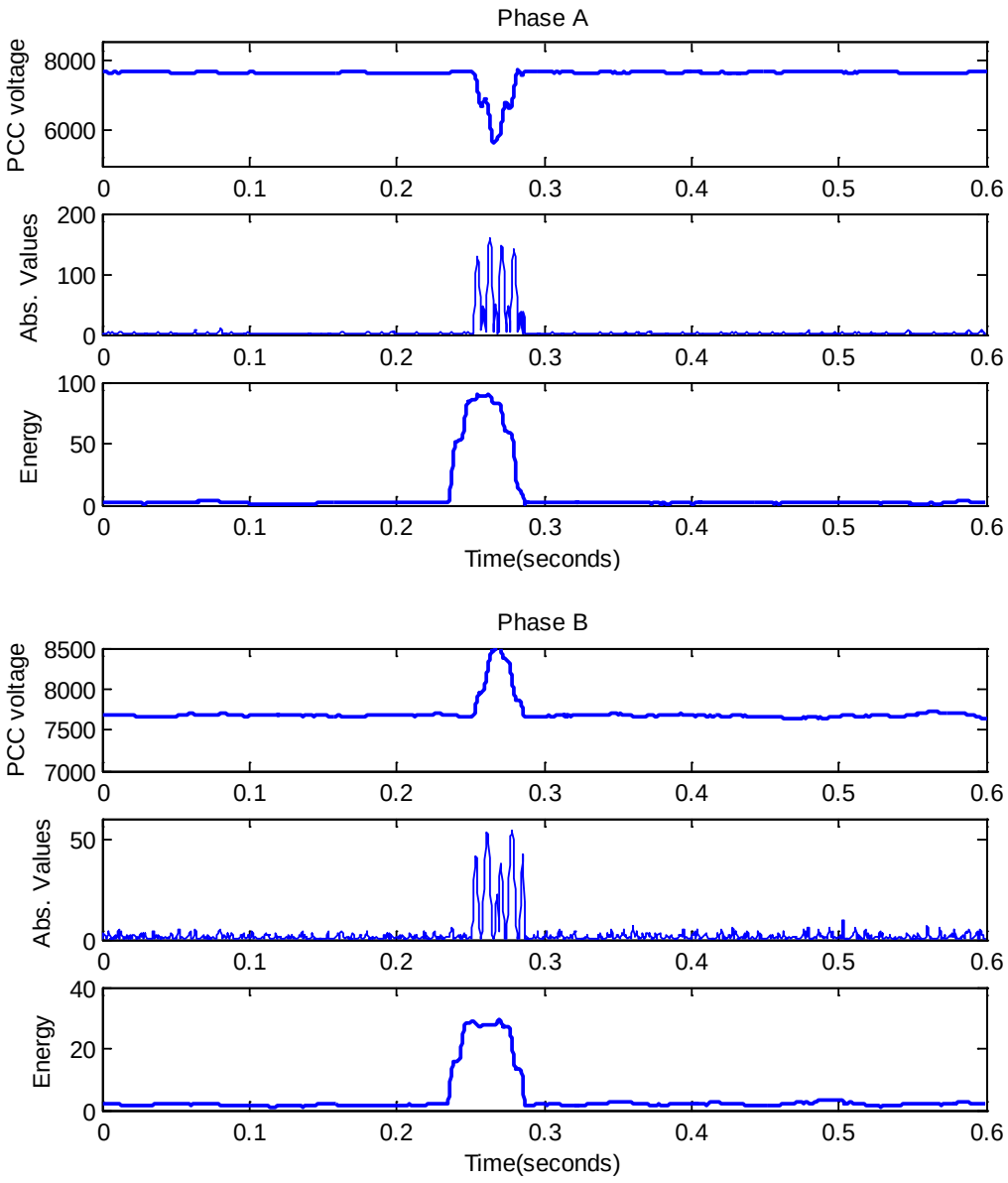

Figure 3.13 Wavelet analysis for Case 3

The above results (Fig. 3.12- Fig. 3.13) show similar behaviors with the 'close to zero' islanding case. First author analyzed the maximum value for different scenarios to see if a pure threshold setting of the fifth level wavelet coefficient and energy content can

be treated as a criterion to distinguish islanding and non-islanding. Table 3.1-3.2 show the maximum value of detail coefficients and corresponding maximum energy content for different cases, respectively.

Table 3.1 Maximum value of detail coefficients for different cases (Level 5)

	Case 1	Case 2	Case 3
Phase a	37.12	31.70	155.5
Phase b	30.12	15.28	53.07
Phase c	37.76	8.893	22.94

Table 3.2 Maximum value of energy content for different cases

	Case 1	Case 2	Case 3
Phase a	19.24	18.81	89.52
Phase b	17.87	7.60	27.95
Phase c	22.36	3.909	11.35

From the above two tables, it is not easy to find a major difference between islanding and other two cases. For example, for islanding in phase a, the maximum of detail coefficient is 37.12, but this value for other two cases in same phase are 31.70 and 155.5. These numbers are totally different and it is hard to find out islanding shows larger variations than other cases, so as energy content. That means it is impossible to set a threshold to distinguish islanding and non-islanding situations so that we can avoid mal-operate. Thus, it verifies the method proposed in [21] - a simple threshold setting of detail coefficients and energy contents, may fail to detect islanding in most cases.

However, from the introduction to wavelet-transform, we know wavelet is extremely sensitive to sudden change. From the figures, we can easily find the results demonstrate this main characteristic of wavelet-transform. In addition, when events (including islanding and non-islanding) occur, the wavelet coefficients and energy content soon reach the maximum value. That means although wavelet-transform method is not adapted to detect islanding, at least it can be used to detect or decide whether event occurs, no matter it is islanding or not. Author will propose a method in next section, to determine the time of event occurrence based on this idea.

Chapter 4 Multi-feature Based ANN Classifier

Since the passive islanding detection methods discussed above have the limitations such as the dependence of the threshold values, author tries to propose a new method related to THD&VU to solve this problem. The aim of our research is to find the hidden regularities in large output data of different islanding and non-islanding cases. Therefore, by reviewing large number of literatures, author finds artificial neural network (ANN) is a good data analysis tool which can be trained to identify relationships from complicated data. Thus the structure of proposed method is that, first using wavelet-analysis to get the sample number event occurs, and then to obtain features extracted from the monitoring parameters in THD&VU method, which we have already studied in the previous chapters, as the inputs of neural network. The effectiveness of the proposed method is tested with a large number of credible islanding and non-islanding cases. Next section presents an introduction to ANN technique briefly and proposed method.

4.1 Brief introduction to ANN classifier

ANN is a widely used statistical learning algorithm in data mining. The basic idea of ANN was inspired by biological neural network such as human brain. Human brain is composed of amount of different neurons which are massively and complicatedly interconnected. ANN has similar structure of human brain, or it is a simplified model of brain and it predicts event by learning knowledge and store it within neuron connection weights [40]. For many complex problems which are hard to solve by traditional computation methods, ANN might be a good idea to instead of. ANN can solve the problems which have following conditions:

1. A problem which has exact input and output data, but it's really hard to relate both.
2. The classification task is very complicated but has a definite answer or output.
3. It is easy to find out a large number of examples of correct output.

For the islanding detection problem in this paper, it is clear that it is very difficult to find a single criterion to differentiate islanding events from other non-islanding events. What's more, it is important to notice that ANN can learn by example because it can learn how to predict outputs based on the given input data by using training algorithm. In this case, it is just easy to provide enough examples which have exact answers for ANN learning. For these reasons, ANN method is selected and supposed to be a good classifier to deal with so many variables.

This paper uses a well-used type of neural network model, which is known as 'feed-forward back-propagation network' (BP network) [41]. Fig. 4.1 shows the basic architecture of ANN. From the figure, we can easily see ANN has three-layer architecture: input nodes, hidden nodes, and output nodes. Each node (neuron) in one layer is connected to each node in the next layer, and if we apply information to the inputs of the first layer, the information will flow across the hidden layer to output layer. The number of nodes in the input layer is the same as the input features in the training dataset, and the number of nodes in the output layer is the same with output classes (in this case we only have one class: islanding). The number of hidden nodes in the middle layer is normally between these two numbers. Please note the number of hidden nodes is very important because both over-setting and under-setting will cause poor training results. Fig. 4.2 demonstrates the structure of a node. From the two figures, we can explain the network

mechanism as following steps: First, the nodes in the previous layer send a signal into next layer, and then a separate weight value is used to multiply each of these signals. Then the summed weighted inputs are passed through a limiting function which limits the output in a fixed range (generally is between 0 and 1). The limiter output is then transmitted to the nodes in the next layer [40].

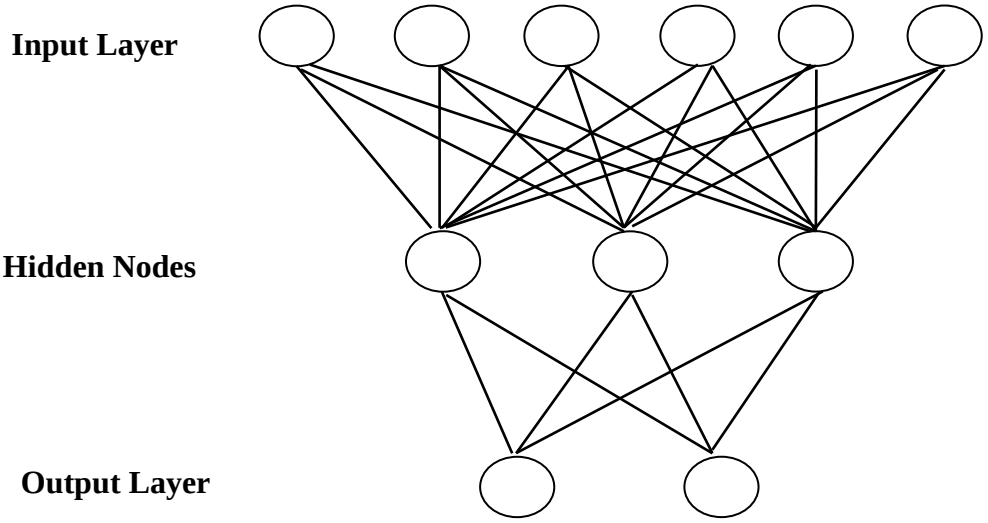

Figure 4.1 basic neural network structure of BP network

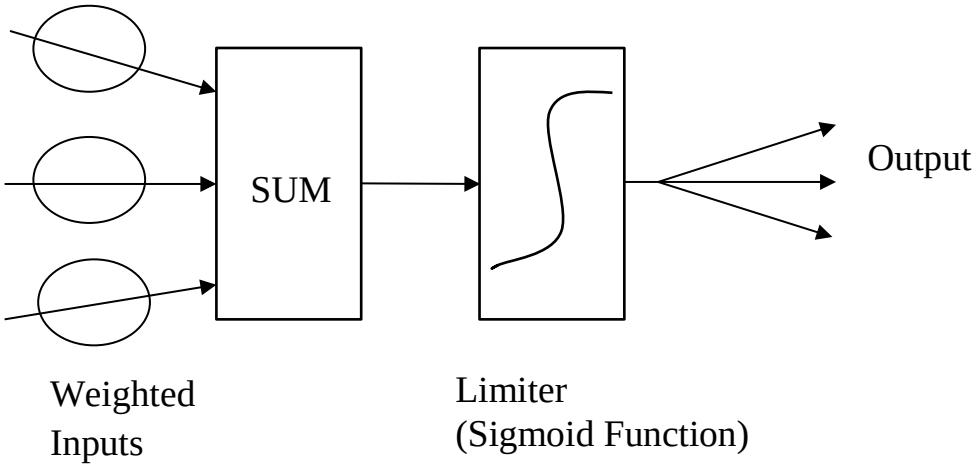

Figure 4.2 Basic structure of a node

Since the intelligent network is based on the weight values between nodes, a method is expected to adjust the weights to adapt to the problem need to be solved. Back

propagation (BP) is such a learning algorithm and is the most common one for this type of network because of its simplicity and validity. Its advantages have been proved in many other applications. Just like what we have already introduced, a BP network needs learning or training process, which means we must provide a set of cases which have exact known output. Then we use these examples to train the ANN so that shows the type of behavior of the network, and BP algorithm make the network adapt to that type of behavior.

The BP learning process achieves the goal in several steps as follows: the first example case is applied to the network, and the network generates some output based on the current state of its weights (generated output is normally random). Then the mean-squared-error (MSE) is calculated in each output neuron. The error value is then propagated backwards through the network, and ANN decides how much changes should be made to the weights in each layer in order to match the generated output with the actual output provided by testing cases. This modification is carried out by the sigmoid transfer function, which determines the output of hidden neuron (Equation 4.1) and that of output neuron (Equation 4.2) [42].

$$f(x_j) = \frac{1}{1+\exp\left(-\left(\sum_{i=1}^{n} X_i \cdot W_{ij} - \theta_{ij}\right)\right)} \tag{4.1}$$

$$f(x_k) = \frac{1}{1+\exp\left(-\left(\sum_{j=1}^{m} X_j \cdot W_{jk} - \theta_{jk}\right)\right)} \tag{4.2}$$

Where, X_i is the input value, W_{ij} is the connection weight between the input and the hidden neuron and W_{jk} is the weight between the hidden neuron and the output neuron, respectively, θ_{ij} and θ_{jk} are bias terms for the ith and kth neuron, respectively; $i, j,$ and k are the number of neurons in each layer.

The whole process is operated for each of training cases until the overall error value reaches the anticipated set. Then we can say ANN has been well-trained and can be used for predicting unknown cases.

4.2 Proposed Method

4.2.1 Selection of window width

A typical window width of 10 cycles of observation period has been considered to extract features, since we try to extract features by taking average value of one cycle of the two monitoring parameters THD&VU over three power cycles right after islanding, and we also need enough window cycles to process wavelet analysis. Therefore, 10 cycles window width is chosen for accuracy. What's more, in our simulation timescale, 10 cycles represent 0.167s in 60 Hz power system. For the proposed method, this time delay is short enough in comparison to IEEE 1574 standard, which says DG must be disconnected within 2s after islanding. Thus, 10 cycles observation period is reasonable.

4.2.2 Decide occurrence moment by wavelet-transform

Since we want to know the exact point when event occurs, this section proposes a method based on wavelet-transform to obtain it. In real-time system, 10 cycles observation period is extracted first. Then next steps can be explained by followings:

1. Extract the voltage signal every 10 power cycles.
2. Wavelet-transform and calculate corresponding energy content.
3. Analyze the energy information and collect all the extrema, then get the absolute value.
4. Find the maximum value E_1 and second maximum value E_2 of the absolute extrema.

5. If $\frac{E_1-E_2}{E_2} > 50\%$, we say E_1 is available and the corresponding point of E_1 is the time of events occur.

The reason why we choose energy content for analyzing instead of wavelet coefficients is that the waveform of energy content is more stable and easy for analysis. The purpose of step 5 is to avoid getting some wrong point from a distorted voltage signal, which may have fluctuation in voltage waveform so that its wavelet energy content also has extrema.

4.2.3 Improvement of THD&VU method

In order to demonstrate the efficacy of THD method, I also used a new parameter referred to the energy content of THD, which is given by [43], as the input of ANN:

$$H_t = \frac{1}{N}\sum_{i=1}^{N} THD_t\,(i) \times 16.7ms \tag{4.3}$$

Where, N is the sampling number of one power cycle (16.7ms), and t is the monitoring time. Physically, H can be understood as the area of THD surrounding with the time axis for one power cycle, shown as follows:

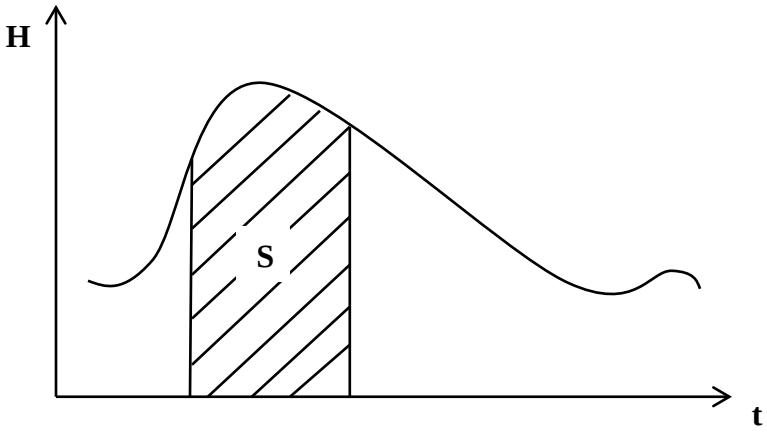

Figure 4.3 the definition of *H*

Thus, we also define the stable value of parameter H as THD:

$$\Delta THD = (THD_{stable} - THD_s)/THD_s$$

$$\Delta H = (H_{stable} - H_s)/H_s \tag{4.4}$$

Then, the three parameters $\Delta THD, \Delta H, \Delta VU$ can be treated as the input of ANN if we do some data processing.

4.2.4 Multi-feature based ANN islanding detection method

The proposed method is a hybrid intelligent ANN approach based on 3 features extracted from PCC. It can be explained in two stages. The first stage is about the training process of ANN with the features obtained under large number of islanding and non-islanding conditions. In the second stage, the trained ANN classifier is applied to detect islanding.

The training and testing procedure can be described as follows:

1. n samples are tested to train the ANN classifier. The PCC voltage of every case is obtained at the end of DG.

2. Three features are extracted by calculating the equations introduced in previous chapters. These features are stored in a feature matrix below

$$F(n) = (\boldsymbol{x_1} \quad \boldsymbol{x_2} \quad \boldsymbol{x_3} \quad \boldsymbol{x_4} \quad \cdots \quad \boldsymbol{x_n})^T$$

$$= \begin{bmatrix} x_{\Delta THD}(1) & x_{\Delta H}(1) & x_{\Delta VU}(1) \\ x_{\Delta THD}(2) & x_{\Delta H}(2) & x_{\Delta VU}(2) \\ x_{\Delta THD}(3) & x_{\Delta H}(3) & x_{\Delta VU}(3) \\ \vdots & \vdots & \vdots \\ x_{\Delta THD}(n) & x_{\Delta H}(n) & x_{\Delta VU}(n) \end{bmatrix} \tag{4.4}$$

3. Every sample x_n belongs to one of the two classes, i.e., $y_n = 1$ represents the islanding and $y_n = 0$ is for non-islanding, so that we can build the class vector corresponding to feature matrix.

4. Train the ANN classifier with the Neural Network Toolbox in MATLAB using feature matrix as the input and class vector as the output.

5. Test the ANN classifier with other samples and the result is obtained as $y_n = 1$ for islanding or $y_n = 0$ for non-islanding.

Then, the islanding detection process in real time with trained ANN is summarized below:

1. PCC voltage signal is extracted every 10 power cycles. De-noise the target signal before sending into ANN classifier.

2. Wavelet-analysis and judge whether event happens.

3. If yes, extract the three features from THD&VU monitoring parameters based on the occurrence moment. And the feature vector is formed as:

$$X_t = \{x_{\Delta THD,} x_{\Delta H}, x_{\Delta vu}\}. \quad (4.5)$$

Where t is the moment when event occurs.

If no, it means no event occurs in this 10 cycle, then repeat 1-3 for next 10 cycle.

4. X_t is classified with the trained ANN classifier and the output $y_n = 1$ for islanding or $y_n = 0$ for non-islanding.

5. If $y_n = 1$, islanding is detected and trip signal is sent, if $y_n = 0$, step 1-5 are repeated for next 10 cycles.

The procedure of real-time islanding detection is shown in Fig 4.4.

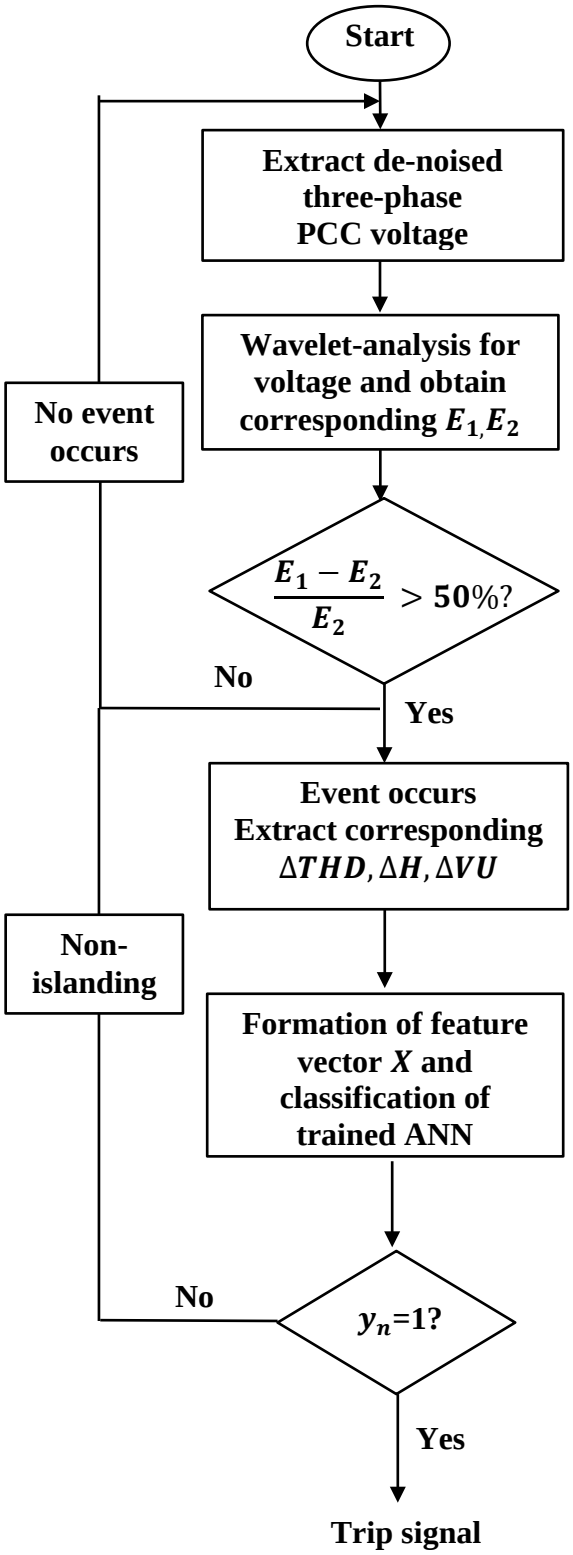

Figure 4.4 Flow chart of proposed method

However, in this thesis, the feasibility of proposed method is examined with large number of offline dynamic events. Therefore, for next section, a training network is simulated and a large set of islanding and non-islanding events are simulated to get the trained ANN classifier. Then several unknown islanding or non-islanding cases are tested to see the selectivity of proposed method.

4.3 Simulation and Results

4.3.1 Events used in training system

In general, we need large amount of different cases to train the ANN classifier. In this paper, author totally uses 6 different types of islanding and non-islanding events in our test system:

1. Trip the circuit breaker to island the distribution generator along with active power mismatch from -30% to 30%. (Large power mismatch cases are not considered here because they can be easily detected with conventional detection methods).
2. Trip the circuit breaker to island the distribution generator along with active power mismatch from -10% to 10% and adjust corresponding reactive power to keep the power factor 0.9.
3. Unbalanced single line to ground faults happen at different positions of the utility grid with different fault resistances.
4. Switching in some loads at different positions of the utility grid, with different active power and reactive power.
5. Introduce pulse disturbances with different magnitudes in utility grid, where is apart from the DG.

6. Switching of capacitor bank connected to the distribution network (in the utility grid) with different capacitive power.
7. Starting induction motor in distribution network with different nominal power and torque.

4.3.2 Case I – Inverter based DG

In this case, only one DG is considered in distribution network. The complete training distribution network is reduced as a single-line diagram, which can be found in Appendix A. The islanding condition can be operated by opening CB1. A list of detailed generated islanding and non-islanding events is shown in Table 4.1.

Table 4.1 Sample List of the Events Under Islanding and Non-islanding Condition

Event Name	Operation	Event Description	No. of events
Islanding	Tripping of CB1,CB2,CB3,CB4	Tripping of CB at different switching time (0.2, 0.21, 0.22 s) with variable power mismatch.	120
Single phase fault	Fuses will open one power cycle after fault 1, 2, 3 are introduced.	Single line to ground faults happen at Phase A at different time and faults are cleared by opening corresponding breaker. Therefore, distribution network will lose this load branch.	30
Switch-in load (SL)	Close CB5,6,7 to switch in SL1,2,3	Switch in load at different time with different power settings.	30
Pulse disturbance (PD)	Introduce PD1,2,3 at target point	Introduce pulse disturbance with different magnitudes,	30
Switch-in capacitor bank	Close CB8 to switch in capacitor bank	Switch in capacitor bank with different capacitive power.	10

From the table, we can see a total of 220 events (including 120 islanding and 100 non-islanding) are generated to train the ANN. For each of these events, the PCC voltage signal was distorted with white noise during generating. Therefore, the distorted signal

needs to be de-noised by using low-pass filter before analysis. In our simulation, the sample rate was 100 kHz and the low-pass frequency for the filter was chosen as 7000 Hz. Then the filtered signal can be used to analysis. After extraction of the three features for each case, the feature matrix was built for the overall 220 events. Then the feature matrix needed to be normalized as the input for training. And the class vector is the output for training. In our study, 2 neurons in hidden layer were selected since the input layer has three nodes and the output layer only has one node. Sigmoid is selected as the transfer function and the trainlm network training function is to be used. Fig 4.5,4.6 shown below demonstrates the training performance.

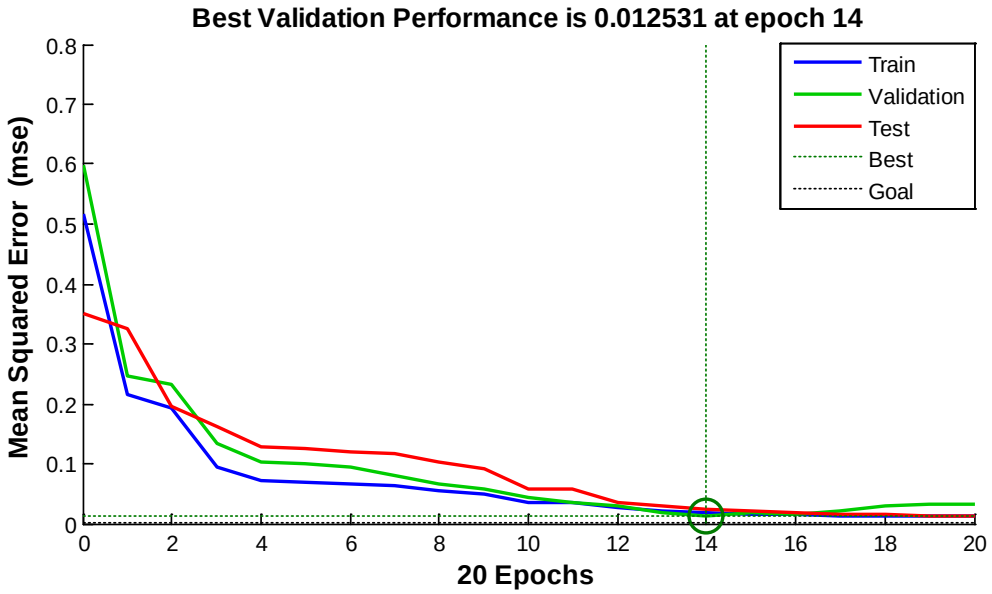

Figure 4.5 Performance of trained ANN for Case 1

From the figure, we can find the algorithm get the best performance at epoch 14.

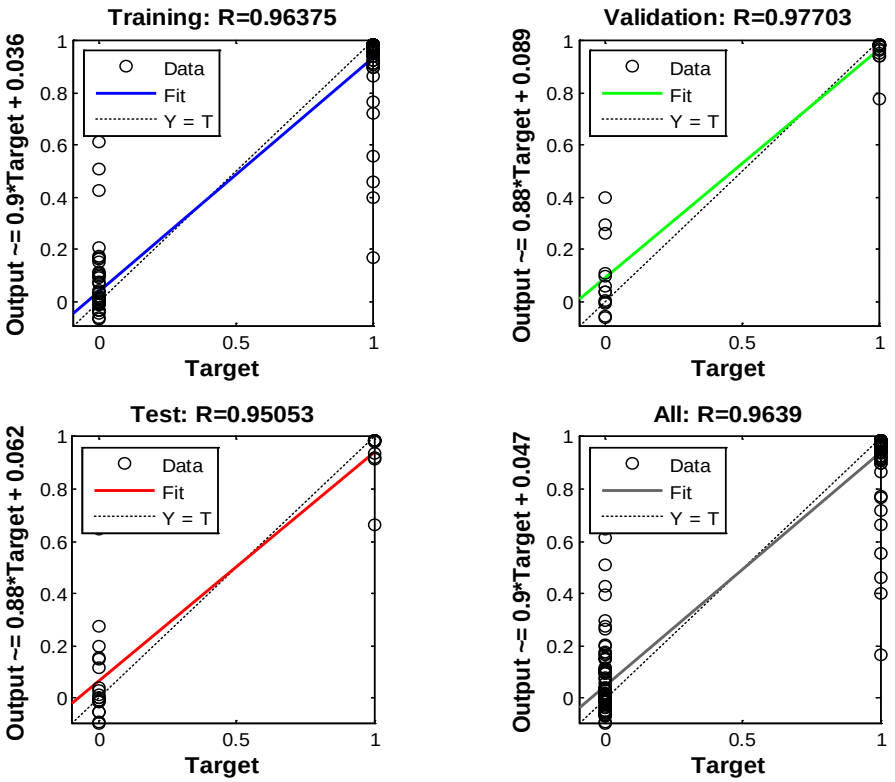

Figure 4.6 Regression of trained ANN for Case 1

Then 35 sample testing events with the same type but different loading conditions are used to test the trained ANN classifier. The purpose of studying unlearned condition is that we are going to see the selectivity of proposed method for unseen cases. The testing distribution network is shown in Appendix B.

Events are: (1) Tripping CB1 to model islanding with different active power. (2) Clear the single line to ground faults with different fault resistance and ground resistance by fusers. (3) Close CB2 to model load switch-in with different load power. (4) Close CB3 and CB4 to model capacitor bank switch-in with different capacitive power. (5) Introduce pulse disturbance at different position. Results of the 35 sample testing events and the resulting parameter indices and the output of algorithm are summarized in Table 4.2.

Table 4.2 Results Obtained From Proposed Algorithm In Case I study

Description	Type	Events Occur(s)	Detection Time(s)	Actual	Output	Test	Error	Trip
Trip CB1	ΔP=-40%	0.21	0.2246	1	1	0.9758	0.0242	1
	ΔP=-24.7%	0.21	0.2160	1	1	0.9353	0.0647	1
	ΔP=-22.5%	0.21	0.2166	1	1	1.0002	0.0002	1
	ΔP=-16.6%	0.21	0.2195	1	1	0.9116	0.0884	1
	ΔP=-13.3%	0.22	0.2253	1	1	0.8036	0.1964	1
	ΔP=-12.2%	0.23	0.2323	1	1	0.8450	0.155	1
	ΔP=-9.7%	0.23	0.2352	1	0	0.3067	0.6933	0
	ΔP=-5.4%	0.23	0.2352	1	1	0.8942	0.1058	1
	ΔP=-2.6%	0.23	0.2352	1	1	0.9262	0.0738	1
	ΔP=1.3%	0.24	ND	1	N/A	N/A	N/A	0
	ΔP=7.9%	0.24	ND	1	N/A	N/A	N/A	0
	ΔP=11.4%	0.24	0.24	1	1	0.9259	0.0741	1
	ΔP=15.6%	0.24	0.2573	1	1	0.9182	0.0828	1
	ΔP=19.3%	0.24	0.2410	1	1	0.8891	0.1109	1
	ΔP=24.7%	0.24	0.2422	1	1	0.9425	0.0575	1
	ΔP=35.6%	0.24	0.2438	1	1	0.9127	0.0873	1
	ΔP=40%	0.24	0.2436	1	1	0.9237	0.0763	1
Fault 1	F=G=15ohms	0.20	0.2058	0	0	0.0756	0.0756	0
	F=G=24ohms	0.20	0.2058	0	0	0.1018	0.1018	0
	F=G=36ohms	0.20	0.2058	0	0	0.0898	0.0898	0
Fault 2	F=G=24ohms	0.21	0.2173	0	0	0.0204	0.0204	0
	F=G=42ohms	0.20	0.2086	0	0	0.0621	0.0621	0
Close CB2	S=400kVA	0.22	ND	0	N/A	N/A	N/A	0
	S=600kVA	0.22	ND	0	N/A	N/A	N/A	0
	S=700kVA	0.22	0.2202	0	0	0.3091	0.3091	0

Close CB3	C=100kVar	0.23	0.23	0	0	0.0062	0.0062	0
	C=200kVar	0.23	0.23	0	0	0.3092	0.3092	0
Close CB4	C=100kVar	0.24	0.241	0	0	0.1867	0.1867	0
	C=130kVar	0.24	0.241	0	0	0.1457	0.1457	0
	C=170kVar	0.24	0.241	0	0	0.1011	0.1011	0
Pulse Disturbance	PD1	0.25	0.2544	0	0	0.0925	0.0925	0
	PD2	0.25	0.2544	0	0	0.0584	0.0584	0
	PD3	0.25	0.2538	0	0	0.0604	0.0604	0
	PD4	0.25	0.2544	0	0	0.1244	0.1244	0
	PD5	0.25	0.2544	0	0	0.0913	0.0913	0
Note: ND=Not detection, PD=Pulse Disturbance								

From the resulting table, we can find the false detection by comparing the values of two columns of this table entitled “actual” and “trip”. The detection accuracy for this case is 91.43% (32 cases over 35 events). We can see this method still has non-detection zone with the influence of noise. For the two cases $\Delta P = 1.3\%\&7.9\%$, the islanding operation is not detected because the change of energy content of wavelet coefficient is too small to satisfy the rule of proposed method. We still can see the proposed method did not detect two load switch-in cases because of the same reason, but the relay sent the right trip signal ‘0’, which did not disconnect the PV DG, so we can’t treat it as misjudge. For the detected situation, only one case is misclassified, which means this method has high reliability and accuracy. All in all, the resulting table demonstrates the proposed method can distinguish most islanding condition with non-islanding, but a small non-detection zone (mostly caused by the distorted voltage signal).

4.3.3 Case II – Inverter-Based DG and Synchronous Generator

In this section, a more complicated case is considered. The study system is shown in Appendix C. This network is same with the previous one except an induction motor and synchronous generator are included. In the study, the nominal power of induction motor is 200 HP and for the SG, the rated power is chosen as 800 kW.

In this case, more events are considered in the training process. (1) Tripping of CB1 to island PV from main grid. (2) Tripping of CB2, CB3, CB4, CB5 to disconnect main source, let SG and PV power the remaining grid alone. (3) Single line to ground fault. (4) Load switching. (5) Introducing pulse disturbance. (6) Capacitor Bank Switching. (7) Turn off induction motor. Table 4.3 shows the sample list used in case 2.

Table 4.3 Sample List for Case 2 Studying

Event Name	Operation	Event Description	No. of events
Islanding	Tripping of CB1,2,3,4,5	Tripping of CB at different switching time (0.2, 0.21, 0.22 s) with variable power mismatch.	120
Single phase fault	Fuses will clear the fault one power cycle after Fault 1, 2, 3 are introduced.	Single line to ground faults happen at Phase A at different time and faults are cleared by opening corresponding breaker. Therefore, distribution network will lose this load branch.	30
Switch-in load (SL)	Close CB6,7,8 to switch in SL1,2,3	Switch in load at different time with different power settings.	30
Pulse disturbance (PD)	Introduce PD1,2,3 at target point	Introduce pulse disturbance with different magnitudes,	30
Switch-in capacitor bank	Close CB9 to switch in capacitor bank	Switch in capacitor bank with different capacitive power.	10
Turn off induction motor	Trip CB10 to turn off induction motor	Turn off 200 HP induction motor with different torque.	10

Figure 4.7, 4.8 show corresponding training results.

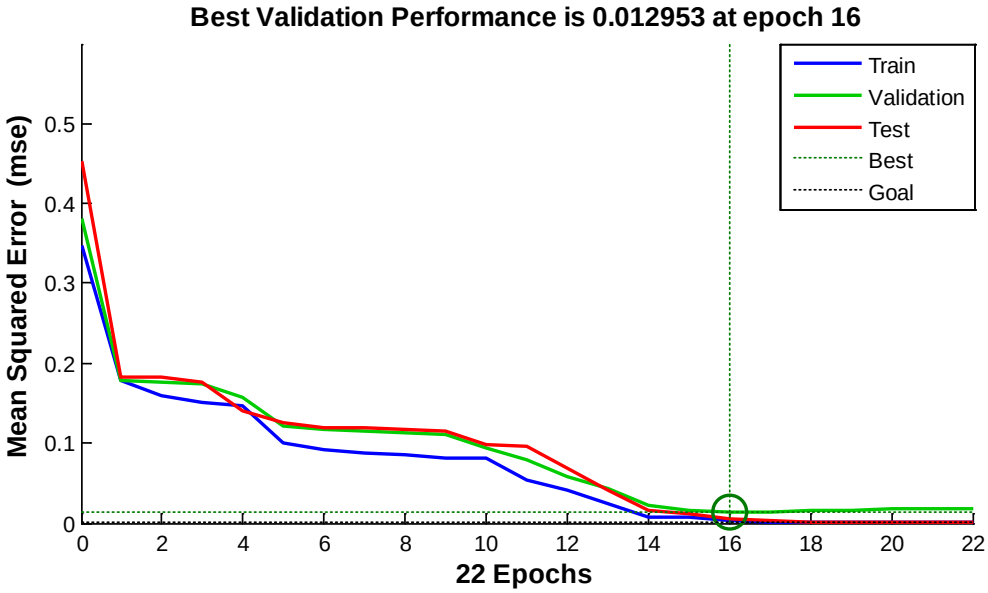

Figure 4.7 Performance for Case 2

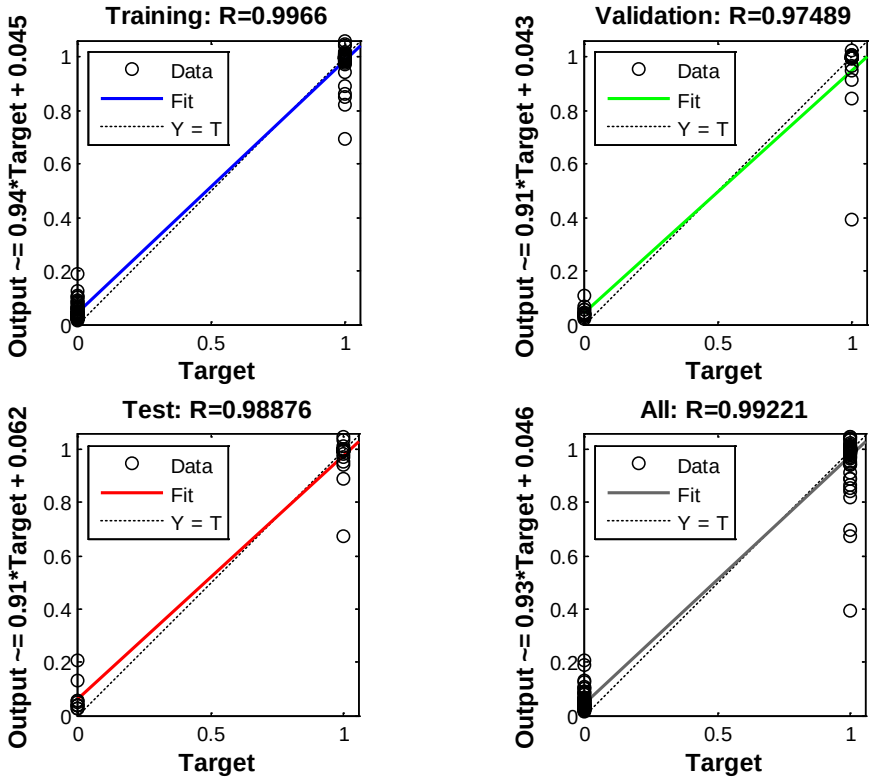

Figure 4.8 Regression for Case 2

Then another 39 sample testing events with the same type but different loading conditions are used to test the trained ANN classifier. The testing distribution network is shown in Appendix D.

Events are: (1) Tripping CB1 and CB2 to model islanding with different active power. (2) Single line to ground faults with different fault resistance and ground resistance were cleared by tripping of fusers. (3) Close CB3 to model load switch-in with different load power. (4) Close CB4 and CB5 to model capacitor bank switch-in with different capacitive power. (5) Introduce pulse disturbance at different position. (6) Turn off induction motor with different torque. Results of the 39 sample testing events and the resulting parameter indices and the output of algorithm are summarized in Table 4.4.

Table 4.4 Results Obtained From Proposed Method in Case 2 Study

Description	Type	Events Occur(s)	Detection Time(s)	Actual	Output	Test	Error	Trip
Trip CB1	ΔP=-39.3%	0.20	0.2083	1	1	0.9961	0.0039	1
	ΔP=-36.2%	0.20	0.2083	1	1	1.0021	0.0021	1
	ΔP=-24.8%	0.21	0.2170	1	0	0.4539	0.5461	0
	ΔP=-18.8%	0.21	0.2176	1	1	0.9545	0.0455	1
	ΔP=-13.2%	0.21	0.2170	1	1	0.9919	0.0081	1
	ΔP=-9.6%	0.22	0.2256	1	1	0.9929	0.0071	1
	ΔP=-6.3%	0.22	0.2256	1	1	0.9954	0.0066	1
	ΔP=-3.7%	0.22	ND	1	N/A	N/A	N/A	0
	ΔP=3.6%	0.22	ND	1	N/A	N/A	N/A	0
	ΔP=10.6%	0.22	0.2272	1	1	0.9090	0.0910	1
	ΔP=14.7%	0.22	0.2259	1	0	0.3702	0.6398	0
	ΔP=19.8%	0.23	0.2326	1	1	0.8210	0.1790	1
	ΔP=23.7%	0.23	0.2342	1	1	1.0123	0.0123	1

	ΔP=30.4%	0.23	0.2342	1	1	1.0066	0.0066	1
	ΔP=35.4%	0.23	0.2342	1	1	1.0149	0.0149	1
	ΔP=41.1%	0.24	0.2426	1	1	0.9945	0.0055	1
Trip CB2		0.20	0.2093	1	1	0.9987	0.0013	1
		0.21	0.2178	1	1	0.9912	0.0088	1
		0.22	0.2245	1	1	0.9934	0.0066	1
		0.23	0.2357	1	1	1.0087	0.0087	1
Fault 1	F=G=15ohms	0.20	0.2125	0	0	0.0280	0.0280	0
	F=G=24ohms	0.20	0.2176	0	0	0.0143	0.0143	0
Fault 2	F=G=24ohms	0.20	ND	0	N/A	N/A	N/A	0
Close CB3	S=400kVA	0.23	ND	0	N/A	N/A	N/A	0
	S=1000kVA	0.23	0.2304	0	0	0.1551	0.1551	0
Close CB4	C=100kVar	0.23	0.2397	0	0	0.0511	0.0511	0
	C=200kVar	0.23	0.2385	0	0	0.0537	0.0537	0
Close CB5	C=100kVar	0.24	ND	0	N/A	N/A	N/A	0
	C=130kVar	0.24	0.2401	0	0	0.0620	0.0620	0
	C=170kVar	0.24	0.2401	0	0	0.0231	0.0231	0
Pulse disturbance	PD1	0.25	0.2550	0	0	0.2799	0.2799	0
	PD2	0.25	0.2550	0	0	0.2663	0.2663	0
	PD3	0.25	0.2550	0	0	0.2484	0.2484	0
	PD4	0.25	0.2550	0	0	0.2663	0.2663	0
Turn off Induction Motor (Trip CB6)	Tm=4.3	0.20	0.2058	0	0	0.0462	0.0462	0
	Tm=5.5	0.20	0.2038	0	0	0.0166	0.0166	0
	Tm=6.7	0.20	0.2038	0	0	0.0065	0.0065	0
	Tm=9.8	0.20	0.2051	0	0	0.0291	0.0291	0
	Tm=13.6	0.20	0.2022	0	0	0.0009	0.0009	0
Note: ND=Not detection, PD=Pulse Disturbance								

By observing the resulting table, the detection accuracy for case 2 is 89.7% (35 cases over 39 events). This result demonstrates that even though a synchronous generator and induction motor were included in the distribution network, the detection accuracy is still guaranteed except 4 false cases in islanding detection. This result also illustrates the proposed method has a small NDZ and the threshold setting for event occurrence need to be discussed carefully. The non-detection phenomenon is also shown in some non-islanding cases, although the final trip signal is right. All in all, the proposed method has high detection accuracy in multi-DG system except the threshold setting of the wavelet method need to be considered again.

Chapter 5 Conclusions

5.1 Summary and Conclusion

With the increasing price of electricity, the huge pressure from the environment, distributed generation will play an important role in future power supply. Although distributed generation offers many benefits, it still faces many problems. Islanding is the most prominent issue among them. This thesis investigated several existed islanding detection methods with the results obtained from MATLAB simulation. The result shows these methods have large non-detection zone with practical noise distorted voltage signal and easily mal-operate with other normal non-islanding operation. Thus, in an attempt to overcome these drawbacks, author proposes a new multi-feature based ANN technique to detect the islanding. In this method, first wavelet-transform is used to detect the time when event (including islanding and non-islanding) is happening. The reason why wavelet-transform is selected is that wavelet is extremely sensitive to the sudden change of signal and here in this case, the energy associated with the wavelet coefficients of the PCC three-phase voltage shows drastic change as soon as event occurs. Thus we can easily detect the time when event happens. After getting the time event occurs, the stable errors of total harmonic distortion and voltage unbalance factor before and after this moment are calculated to obtain the feature vector as the input of ANN classifier. Then ANN will determine whether this event is islanding or not.

The performance and robustness of the proposed method was tested with a large number of islanding and non-islanding conditions. The simulation results show high accuracy and robustness against the noise in voltage signal. The test cases also included

unlearned operation conditions and the resulted accuracy demonstrates the high robustness of the proposed islanding detection method in judging the unseen conditions. Thus, in terms of dependability, accuracy and sensitivity to unbalanced system and the size of NDZ, the proposed transient based ANN technique shows better results than other passive islanding detection methods.

5.2 **Future work**

Although the advantage of proposed method has been identified in this thesis, on the other hand, there are also many drawbacks for this method. Since islanding detection relies on the ANN classifier which is trained by examples, the classifier has to be retrained if the network of distributed generation connected is largely changed, such as addition of large branch of load, connected with more DGs. The process of retraining is also overly complex if a large set of different events are implemented to get the feature matrix. The threshold of wavelet detection is also needed to be changed. Thus, a more reliable general algorithm of calculating the occurrence time is preferred in the future. What's more, for the inverter based distributed generation, only PV generator was considered and simulated in this thesis, thus in future research, other DG technologies like wind turbine, fuel cell or battery storage can be studied to see the performance of proposed method.

The result of the thesis entirely relies on the simulation results. Therefore, for future work, proposed method can be tested on a real micro-grid system to see its performance. I think it is a necessary step for practical application.

A better designed DG system is expected for providing a more stable network. For example, improved VSC would reduce the voltage unbalance and harmonic in the system.

Furthermore, since the proposed algorithm is a passive method, a hybrid method along with active method is also expected to be implemented in the near future.

APPENDIX A: Training Events Used in Case I

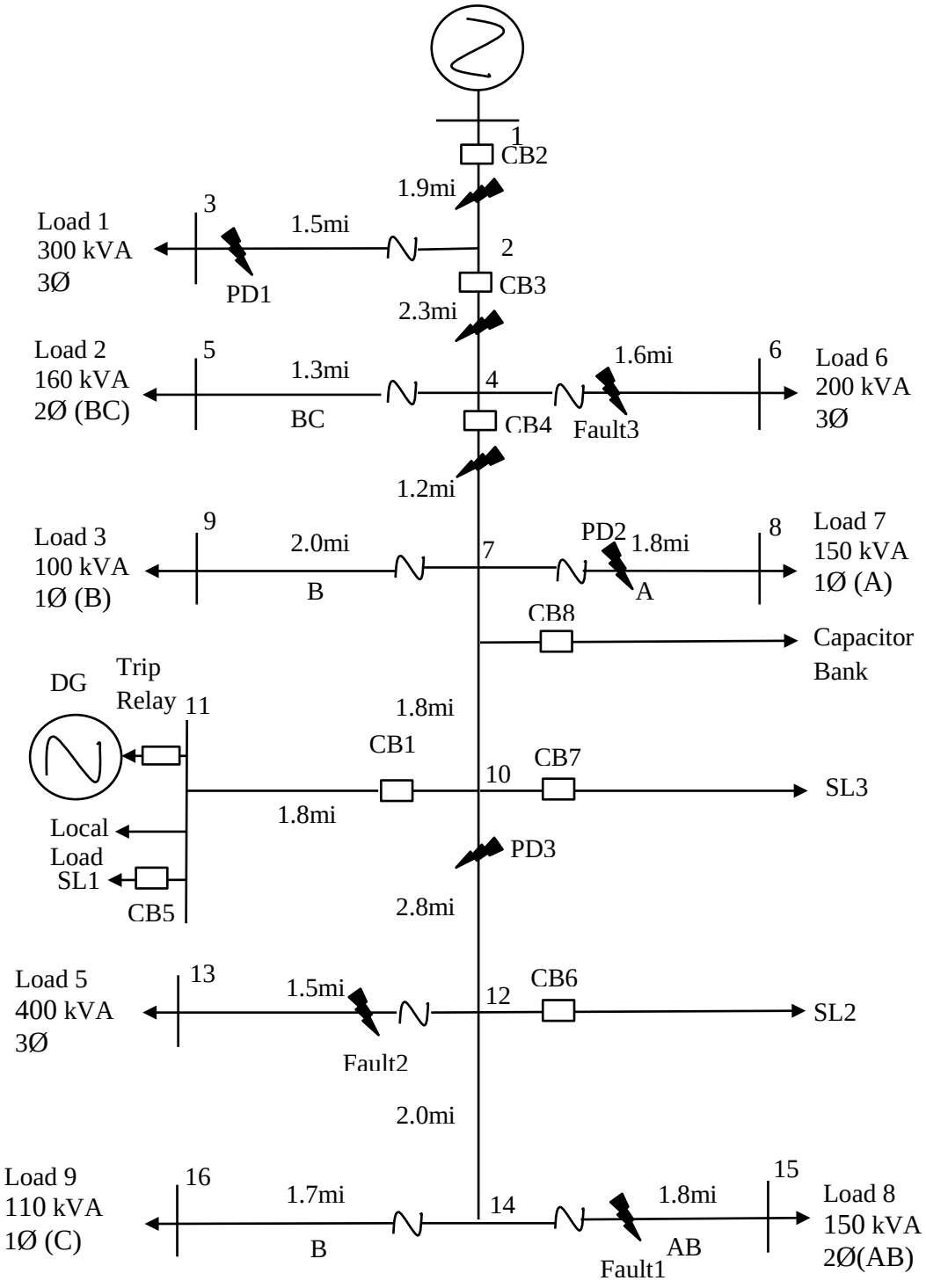

APPENDIX B: Testing Events Used in Case I

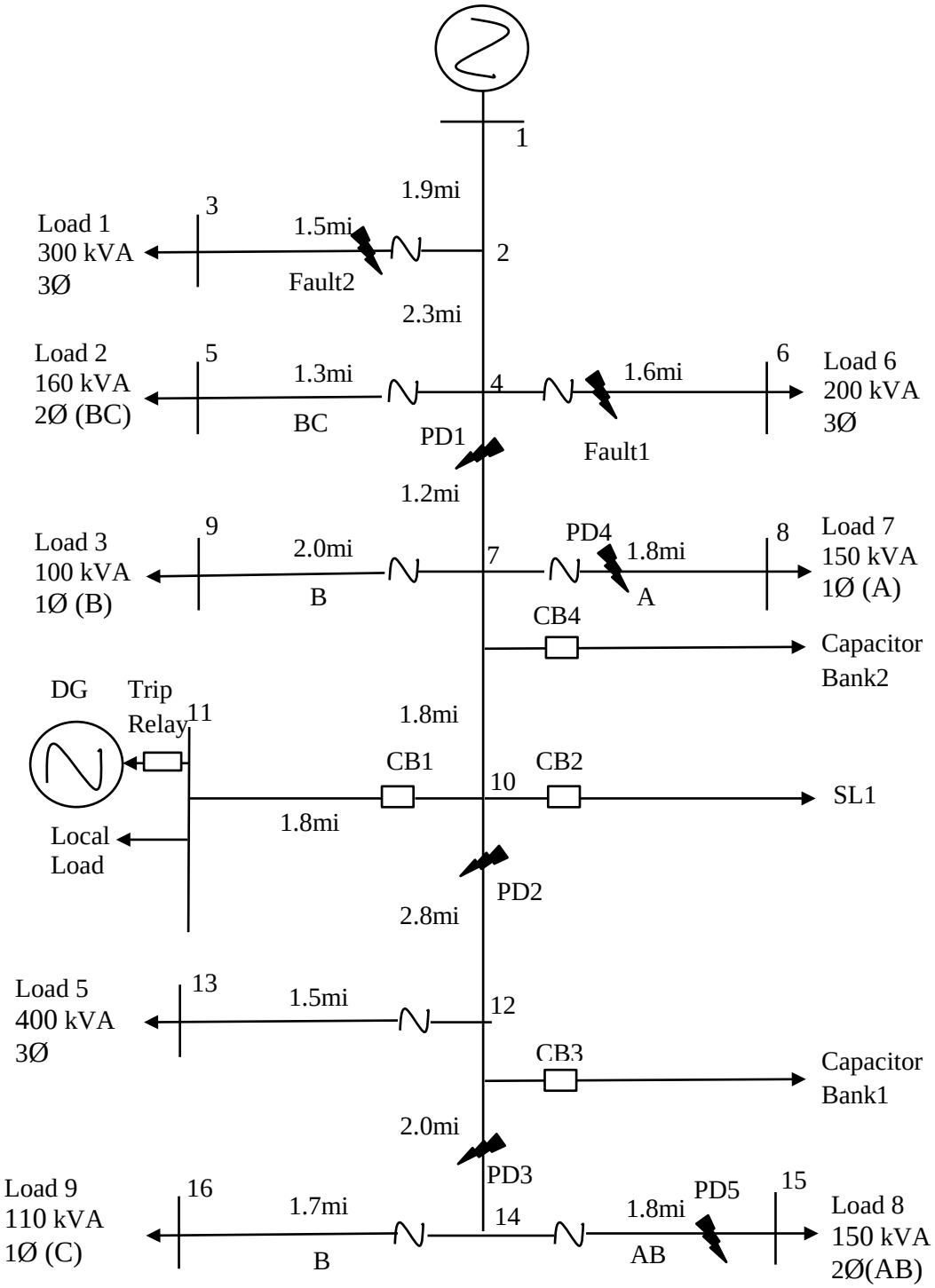

APPENDIX C: Training Events Used in Case II Study

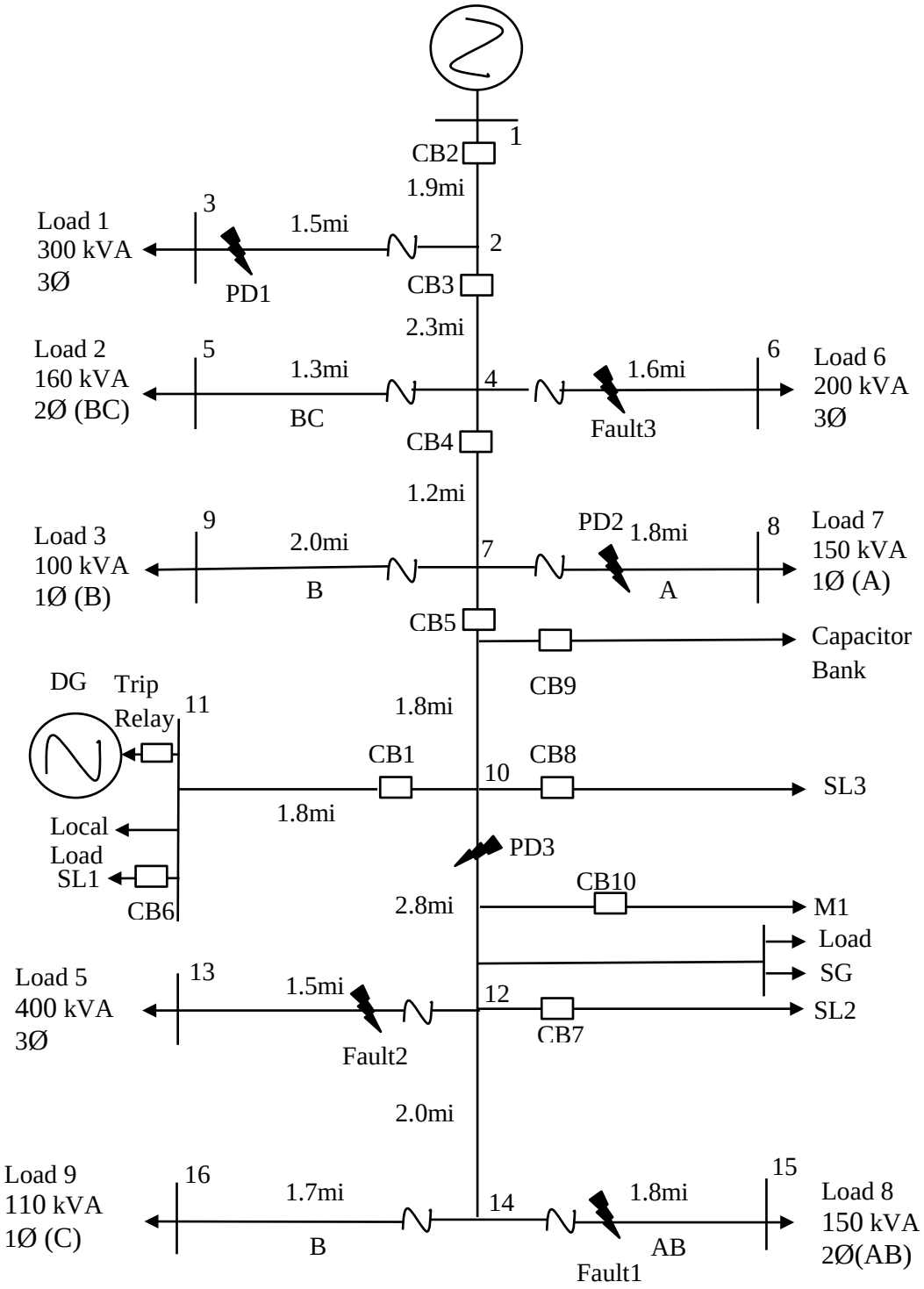

APPENDIX D: Testing Events Used in Case II Study

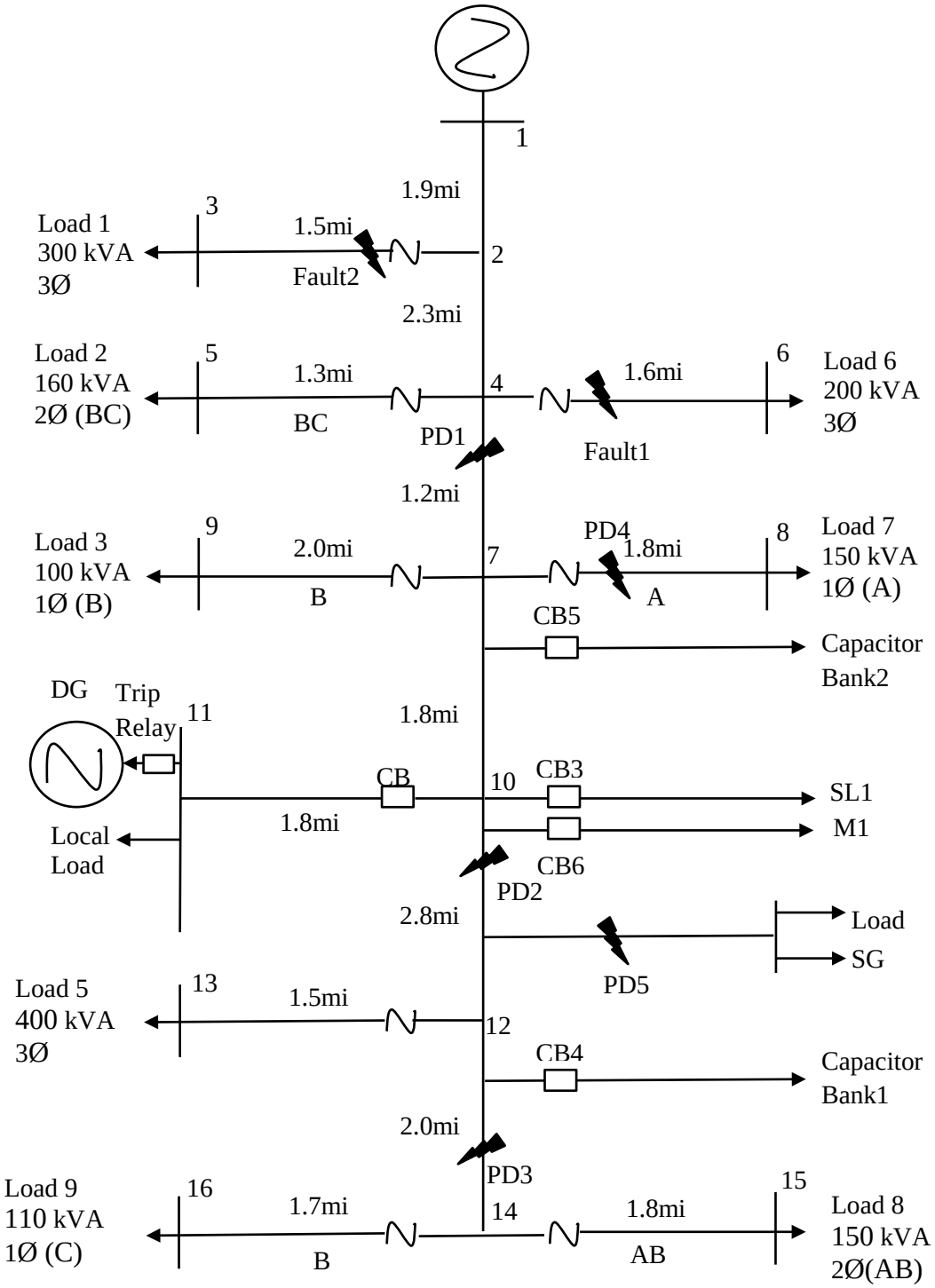

Reference

[1] Yuan Liao, Wen Fan, Aaron Cramer, Paul Dollof, Zongming Fei, Meikang Qui, Siddhartha, Bhattacharyya, Larry Holloway, Bob Gregory, "Voltage and Var Control to Enable High Penetration of Distributed Photovoltaic Systems," in *North American Power Symposium (NAPS)*, Sept. 2012.

[2] S.P. Chowdhury, Chui Fen Tenm, O.A. Crossley, "Islanding Protection of Distribution Systems with Distributed Generators- A Comprehensive Survey Report," in *Power and Energy Society General Meeting- Conversion and Delivery of Electrical 2002 Energy in the 21st Century*, July 2008.

[3] "IEEE Standard 929-2000," *Recommended Practice for Utility Interconnected Photovoltaic (PV) Systems,* 2000.

[4] "IEEE Standard 1574TM," *IEEE Standard for Interconnecting Distributed Resources into Electric Power Systems,* June 2003.

[5] Xu W., Zhang G., Li C., Wang W., Wang G., Kliber J, "A power line signaling based technique for anti-islanding protection of distributed generators-Part I: scheme and analysis," *IEEE Trans. Power Delivery*, vol. 22, no. 3, pp. 1758-1766, 2007.

[6] Yuan Liao, Matthew Turner, and Yan Du, "Development of a Smart-grid Roadmap for Kentucky," *Electric Power Components and Systems,* vol. 42, no. 3, pp. 267-279, 2014.

[7] B., Bozoki, "Effects of noise on transfer-trip carrier relaying," *IEEE Trans. Power Apparatus System,* vol. 87, no. 1, pp. 173-179, 1968.

[8] G. A. Smith, P. A. Onions, D. G. Infield, "Predicting Islanding operation of grid connected PV inverters," *IEEE Proc. Electric Power Applications,* vol. 147, pp. 1-6, Jan. 2000.

[9] M. E. Ropp, M. Begovic, A. Rohatgi, "Analysis and performance assessment of the active frequency drift method of islanding prevention," *IEEE Tran. Energy Conversion,* vol. 14, no. 3, pp. 810-816, Sep. 1999.

[10] W. Freitas, W. Xu, C. M. Affonso, and Z. Huang, "Comparative analysis between ROCOF and vector surge relays for distributed generation applications," *IEEE Trans. Power Del.*, vol. 20, no. 2, pp. 1315-1324, Apr. 2005.

[11] G . Hung, C. Chang, and C.Chen, "Automatic phase-shift method for islanding detection of grid-connected photovoltaic inverter," *IEEE Trans. Energy Convers*, vol. 18, no. 1, pp. 169-173, Mar. 2003.

[12] A Samui, S.R.Samantaray, "Assessment of ROCPAD Relay for Islanding Detection in Distributed Generation," *IEEE Trans. Smartgrid*, vol. 2, no. 2, pp. 391-398, Jun. 2011.

[13] Arachchige, Lidula Nilakshi Widanagama, "Determination of Requirement for Smooth Operating Mode Transition and Development of a Fast Islanding Detection Technique for Microgrids," *Ph.D. dissertation,* vol. Dept. Elec. and Com. Eng., no. Univ. of Manitoba, pp. Winnipeg,MB, 2012.

[14] Andrew J. Roscoe, Graeme M. Burt, and Chris G. Bright, "Avoiding the Non-Detection Zone of Passive Loss-of-Mains (Islanding) Relays for Synchronous Generation by Using Low Bandwidth Control Loops and Controlled Reactive Power

Mismatches," *IEEE Transactions on smart grid*, vol. 5, no. 2, March 2014.

[15] Sami Alshareef, Saurabh Talwar, Walid. G. Morsi, "A New Approach Based on Wavelet Design and Machine Learning for Islanding Detection of Distributed Generation," *IEEE Transaction on smart grid*, vol. 5, no. 4, July 2014.

[16] Omar N. Faqhruldin, Ehab F. El-Saadany and Hatem H. Zeineldin, "A Universal Islanding Detection Technique for Distributed Generation Using Pattern Recognition," *IEEE Transactions on smart grid*, vol. 5, no. 4, July 2014.

[17] Mohamed Al.Hosani, Zhihua Qu, H. H. Zeineldin, "Development of Dynamic Estimators for Islanding Detection of Inverter-Based DG," *IEEE Transactions on Power Delivery*, vol. 30, no. 1, Feb. 2015.

[18] Chun Li, Jason Savulak, and Robert Reinmuller, "Unintentional Islanding of Distributed Generation--Operation Experience From Naturally Occured Events," *IEEE Transactions on Power Delivery*, vol. 29, no. 1, FEB 2014.

[19] M.R.Alam, K.M.Muttaqi,and A. Bouzerdoum, "A Multifeature-Based Approach for Islanding Detection of DG in the Subcritical Region of Vector Surge Relays," *IEEE Transactions on Power Delivery*, vol. 29, no. 5, Oct. 2014.

[20] S. I. Jang, and K. H. Kim, "An islanding detection method for distributed generations using voltage unbalance and total harmonic distortion of current," *IEEE Trans. Power Delivery*, vol. 19, no. 2, pp. 745-752, April 2004.

[21] M. Hanif, U.D Dwivedi, M.Basu, K. Gaughan, "Wavelet Based Islanding Detection of DC-AC Inverter Interfaced DG systems," in *UPEC2010*, 2010.

[22] Liaoyuan, "A novel method for locating faults on distribution networks," *Electric*

Power Systems Research, vol. 117, pp. 21-26, 2014.

[23] Mahadeva, Ramachandran Tripunithura, "Islanding Issues Associated With Photovoltaic Inverters," *Ms. thesis,* vol. Dept. Elec. and Com. Eng., no. Univ. of Nevada, p. Las Vegas, December, 2005.

[24] Moacyr A. G. de Brito, Leonardo P. Sampaio, Luigi G. Jr., Guilherme A. e Melo, Carlos A. Canesin, "Comparative Analysis of MPPT Techniques for PV Applications," in *2011 International Conference on Clean Electrical Power (ICCEP),* 2011.

[25] Pierre Giroux, Gilbert Sybille, Carlos Osorio, Shripad Chandrachood, "Detailed Model of a 100-kW Grid-Connected PV Array," 2014. [Online]. Available: http://www.mathworks.com/help/physmod/sps/examples/detailed-model-of-a-100-kw-grid-connected-pv-array.html.

[26] Kunte, Rohit S, "A Wavelet Transform-Based Islanding Detection Algorithm for Inverter Assisted Distributed Generations," *M.S. Thesis,* Vols. Tennessee Technological University, TN, p. ECE, 2009.

[27] Ropp, W.Bower and M., "Evaluation of Islanding Detection Methods for Photovoltaic Utility-Interactive Power System," *Tech Rep. IEA PVPS T5-09,* 2002.

[28] Z., Ye; al, et, "Evaluation of Anti-islanding Schemes based on Nondetection Zone Concept," *IEEE Trans. Power Electronics,* vol. 19, no. 5, Sept 2004.

[29] EN50438, "Requirements for the connection of micro-generators in parallel with public low-voltage distribution network," in *European Committee for Electro technical Standardization,* December 2007.

[30] Arfat Siddique, G.S. Yadava and Bhim Singh, "Effects of Voltage Unbalance on Induction Motors," in *Conference Record of the 2004 IEEE International Symposium on Electrical Insulations,* Indianapolis,IN, USA, 2004.

[31] Moreau, Iaroslav Blagouchine and Eric, "Analytic Method for the Computation of the Total Harmonic Dostortion by the Cauchy Method of Residues," *IEEE Transactions on Communications,* vol. 59, no. 9, pp. 2478-2491, Sep. 2011.

[32] U. D. Dwivedi, S.N. Singh, "De-noising Techniques with Change Point Approach for Wavelet-Based Power Quality Monitoring," *IEEE Transactions on Power Delivery,* vol. 24, no. 3, pp. 1719-1727, 2009.

[33] U. D. Dwivedi, S.N. Singh,and S.C. Srivastava, "A Wavelet based Approach for Classification and Location of Faults in Distribution Systems," *IEEE Conf. & Exhibition on Control, Communication and Automation,* vol. 2, pp. 488-493, 2008.

[34] Daubechies, J., "The wavelet transforms, time frequency localization and signal analysis," *IEEE Transaction IT,* vol. 36, no. 5, pp. 961-1005, 1990.

[35] M. R. Vatani, M. J. Sanjari, G. Gharehpetian, M. Noroozian, "A New Fast and Reliable Method for Islanding Detection Based on Transient Signal," in *2nd Iranian Conference on Smart Gird,* Tehran, Iran, 212.

[36] U. D. Dwivedi, S.N. Singh, "Enhanced Dectection of Power Quality Events Using Intra and Inter-scale Dependencies of Wavelet Coefficients," *IEEE Transactions Power Delivery,* vol. 25, no. 1, pp. 358-366, 2010.

[37] D.C. Robertson, O.I. Camps, J.S. Mayer, and W.B. Gish, "Wavelets and Electromagnetic Power System Transients," *Proc. IEEE Transactions on Power*

Del., vol. 11, no. 2, Apr. 1996.

[38] Chen, S., "Feature Selection for Identification and Classification of Power Quality Disturbances," *Power Engnineering Society General Meeting,* vol. 3, pp. 2301-2306, 2005.

[39] V.V. Garcia, C.A.D Gualdron and G.O. Plata, "Obtaining patterns for classification of power quality disturbances using biorthogonal wavelets,RMS value amd support vector machines," *EPQU 2007,* pp. 1-6.

[40] Kim, Jun Ha, "Artificial Neural Network Based Decision Support Model For Alternative Workplace Arrangements: Readiness Assessment and Type Selection," *Ph. D. Dissertation,* vol. Georgia Institude of Technology, p. College of Architecture, 2009.

[41] Arthur Earl Bryson, Yu-Chi Ho, in *Applied Optimal control:Optimization, estimation, and control.*, Blaisdell Publishing Company or Xerox College Publishing, 1969, p. 481.

[42] Kim, G.H., An, S.H. and Kang, K.I., "Comparison of construction cost estimating models based on regression analysis, neural networks, and case-based reasoning," *Building and Environment,* vol. 39, pp. 1235-1242, 2004.

[43] Ma Jing, Mi Chao, Wang Zengping, "A Novel Islanding Detection Method Based on Positive Feedback of Voltage Harmonic Distortion," *Automation of Electric Power Systems,* vol. 36, no. 1, pp. 47-49, 2012.

VITA

Education

08/2013— 05/2015

Master Student

Department of Electrical and Computer Engineering, University of Kentucky, Lexington, Kentucky, USA

09/2008—07/2012

Bachelor of Engineering

Electrical and Computer Engineering, Majored in Automation, University of Shanghai for Science and Technology (USST), Shanghai, P. R. China

Awards

08/2013—05/2014

PEIK Scholarship, Power and Energy Institute of Kentucky (PEIK), University of Kentucky, Lexington, KY, USA

09/2008—07/2012

Student Scholarship, USST, Shanghai, P. R. China